

COMPUTATION OF PSEUDOSONIC LOGS IN SHALLOW FRESH/BRACKISH

WATER WELLS:

A TEST CASE

IN

BRUNSWICK, GEORGIA

by

Nancy J. Allen

Thesis submitted to the Faculty of the
Virginia Polytechnic Institute and State University
in partial fulfillment of the requirements for the degree of

Master of Science

in

Geophysics

APPROVED:

Edwin S. Robinson, Chairman

Cahit Çoruh

John K. Costain

November 13, 1989

Blacksburg, Virginia

COMPUTATION OF PSEUDOSONIC LOGS IN SHALLOW FRESH/BRACKISH

WATER WELLS:

A TEST CASE

IN

BRUNSWICK, GEORGIA

by

Nancy J. Allen

Edwin S. Robinson, Chairman

Geophysics

(ABSTRACT)

Due to the usefulness of sonic logs in formation evaluation, efforts have been made to develop a method for calculating pseudosonic logs for wells in which sonic logs were not originally obtained. These efforts attempt to use electrical resistivity data in the calculation of pseudosonic logs by means of empirical scale functions. The purpose of this study is to examine ways of applying these relationships in relatively shallow wells where the principal formation fluid is fresh or brackish water. Data from four wells situated in Brunswick, Georgia were used in this study.

Conventional focused resistivity logs are sensitive to beds as thin as one foot and can provide detail similar to that seen on sonic logs. Focused resistivity logs should be best for conversion to pseudosonic logs in shallow wells, where invasion is minimal and the water used for drilling fluid has electrical resistivity close to that of formation water. Sonic and resistivity logs from a representative well are needed in the procedure for finding an empirical relationship between sonic transit time and resistivity. Values of transit time plotted versus resistivity are read from corresponding depths on both types of logs. The graphs obtained in this study reveal significantly more scatter than previously published graphs based upon deep well data.

An important feature clearly evident in the graphs is the presence of groups of points which are offset from each other. A separate scale function relating transit time and resistivity can be obtained

from each group of points. It is noted that the different groups correspond to differences in the chlorinity of the formation water. The results of this study indicate that it is necessary to consider the salinity of the formation water as well as electrical resistivity for purposes of calculating pseudosonic logs. In previous studies three constant coefficients were determined experimentally in order to obtain an empirical scale function. The present study suggests that it may be possible to replace these constants with chlorinity dependent coefficients. The final results of this study indicate that reasonably reliable pseudosonic logs can be obtained only by using high quality focused resistivity logs from wells where information about the salinity of the formation water is also available.

Acknowledgements

I would like to express my gratitude to the Georgia Water Resources Division and for giving me the opportunity to work on this project. Many sincere thanks go to Dr. Edwin Robinson, my major advisor, for his expert knowledge and guidance. I also want to thank him for sharing his technical writing and editing skills with me during the course of my thesis research. I value and greatly appreciate the technical expertise provided by Dr. Cahit Coruh and Dr. John Costain. I want to thank both of them for initially helping me obtain this project and the funding from the Georgia Water Resources Division.

I also wish to thank all the staff and my fellow graduate students in geophysics for their help and suggestions offered during the course of my stay at Virginia Tech. Among the graduate students I especially wish to give my personal and heartfelt thanks to for their special assistance are

(Phd), (Phd), (Phd), (Phd candidate), and

(Phd candidate). Others I wish to acknowledge for their help in this study are

and from the Georgia Water Resources Division, (Phd in

geology), and the following people from Amoco Production Company,

, and . Finally, I wish to dedicate this thesis to my family who have always believed in me.

Table of Contents

INTRODUCTION	1
BASIS FOR PSEUDOSONIC LOGS	3
Qualitative Correlation of Sonic logs and Resistivity logs	3
Dependence of velocity and transit time on porosity	5
Dependence of resistivity on porosity	7
Scale functions	9
CONVENTIONAL WELL LOGS	11
Sonic logs	11
Resistivity logs	11
The invaded zone	13
Smoothing	15
TEST WELLS	17
Geologic Setting	17
Description of test wells	19

PSEUDOSONIC LOGS	22
Transit time versus resistivity plots	22
Scale functions	27
Pseudosonic logs for the test wells	31
 SUMMARY AND CONCLUSIONS	 39
 BIBLIOGRAPHY	 42
 Appendix A. PSEUDOSONIC AND SONIC LOGS FOR ALL FOUR TEST WELLS IN BRUNSWICK, GEORGIA.	 44
 VITA	 65

List of Illustrations

Figure 1. Sonic and resistivity log comparison	4
Figure 2. Illustration of a scale function curve	10
Figure 3. Conventional non-borehole compensated device	12
Figure 4. Electrode configurations	14
Figure 5. Borehole environment with invaded zone	16
Figure 6. Map of well field with chloride concentration contours	18
Figure 7. Generalized stratigraphic column for TW26	20
Figure 8. Plot of Grant St. logs	21
Figure 9. TT vs. R plots	23
Figure 10. TT vs. R plots for TW26	24
Figure 11. TT vs. R plots	26
Figure 12. Sonic vs. Pseudosonic (TW26)	32
Figure 13. Sonic vs. Pseudosonic (Grant St.)	34
Figure 14. Sonic vs. Pseudosonic (Hercules 'O')	35
Figure 15. Sonic vs. Pseudosonic (BP&P 10)	36

List of Tables

Table 1. Velocities and transit times for typical minerals and sedimentary rocks.	6
Table 2. Resistivities of common minerals and sediments	8
Table 3. Values of A, B, and C for each of the scale function in the TW26, Hercules 'O', Grant St., and BP&P No. 10 Wells	30
Table 4. Correlation coefficients or Pearson's r at zero lag for all four test wells.	38

INTRODUCTION

The sonic log has become an important tool for borehole formation evaluation. It is especially useful for porosity estimation, as well as for lithologic correlation, and to aid in the interpretation of seismic surveys. Unfortunately, sonic logging has not been done in a large number of wells for which conventional electric logs are available. To overcome this deficit, methods have been proposed for using these electric logs in the calculation of pseudosonic logs (Rudman, 1984). These calculations have been done with logs from oil and gas wells where saline water is the principal formation fluid. The object of this study is to adapt these methods for calculation of pseudosonic logs in fresh/brackish water wells.

Empirical relationships between electrical resistivity, sonic transit time, and porosity provide the basis for calculating pseudosonic transit time. These relationships can be established by analysis of resistivity and sonic logs from the same well. Test logs available for this study are from four wells located near Brunswick, Georgia that range from 865 feet to 2720 feet in depth. In addition, chemical analyses of fresh/brackish water samples and a chlorinity log from one of these wells provides information for assessing the effect of groundwater salinity in the calculations of pseudosonic logs. Salinity, which has an important effect on resistivity, has not been treated quantitatively in earlier calculations.

This report begins with a review of the factors involved in pseudotransit time calculations, the logging methods used to obtain the data for these calculations, and the methods for determining a resistivity - transit time scaling function. It continues with a description of test wells and logs near Brunswick, Georgia, and the calculation of pseudosonic logs for these wells. The quality of these pseudosonic logs is then examined by qualitative comparison and quantitative cross-correlations, with measured sonic logs.

BASIS FOR PSEUDOSONIC LOGS

Qualitative Correlation of Sonic logs and Resistivity logs

Comparison of sonic and electrical resistivity logs typically reveals an inverse relationship. This is seen in Figure 1 where relatively high sonic transit times correspond to zones of relatively low resistivity. This correlation together with the similarity of relative amplitude variations suggested the possibility of using resistivity logs for the calculation of pseudosonic logs. However, the correspondence of closely spaced amplitude variations is affected by the sensor configurations of the logging tools. It is clear from Figure 1 that the 16 inch normal log is insensitive to the thin zones that were detected by both the focused resistivity log and the sonic log for which the sensors are spaced at intervals of 12 inches and 2 feet respectively. This indicates that if closely spaced amplitude variations ordinarily seen on sonic logs are used to establish relationships between resistivity and transit time, the logs should be smoothed to insure that these values represent more or less the same zone in a formation.

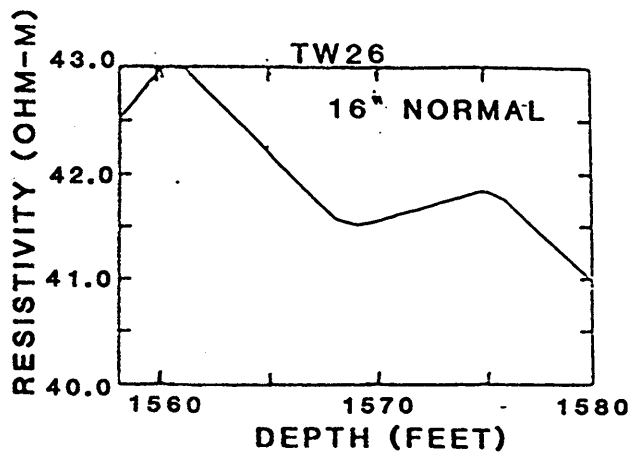
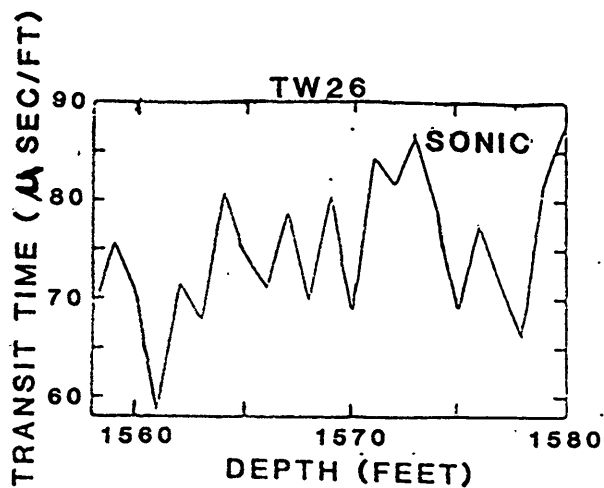
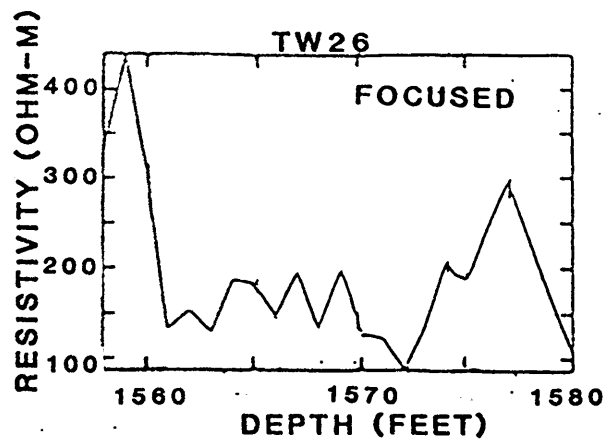


Figure 1. Sonic and resistivity log comparison: Example of a section of the focused, 16" normal resistivity and sonic logs from TW26.

Dependence of velocity and transit time on porosity

Certain properties affect the acoustic velocity or transit time in a formation as well as the electrical resistivity. Factors having the most important effect on velocity or transit time in a formation are the compositions of the solid matrix and the formation fluid, and the proportions of solid and fluid which are specified by the porosity. The dependence of velocity or transit time on composition can be judged from the values given in Table 1 for some common minerals and sedimentary rocks. These values also depend on temperature and pressure, but the effects on the solid part are small enough to neglect for the temperature and pressure ranges incurred in the test wells used in this study.

In formation fluids the acoustic velocity tends to be much lower, and the corresponding transit time much higher than in the solid part of the formation. According to Knauss (1978), the acoustic velocity in saline water can be found from the formula:

$$V_w = 1449 + 4.6T - 0.055T^2 + 0.0003T^3 + (1.39 - 0.012T)(S - 35) + 0.017Z \quad (1)$$

where the acoustic velocity (V_w) is in m/s, temperature T in degrees C, the depth Z in meters which accounts for pressure, and the salinity S in grams/liter. The brackish and saline water in the test wells used in this study have approximately the same proportion of chloride to total salinity that exists in seawater. Therefore, salinity can be estimated directly from chlorinity using the formula (Knauss, 1978):

$$\text{salinity} = 1.80655 \times \text{chlorinity} \quad (2)$$

For the ranges of salinity, temperature, and depth encountered in these wells the acoustic velocity would be in the range between 1440 m/s (4720 ft/s) and 1580 m/s (5180 ft/s). This range is close to that given in Table 1 for the water and mud filtrate commonly found in deep oil wells. The values found from these equations and the data in Table 1 indicate that acoustic velocity or transit

Table 1. Velocities and transit times for typical minerals and sedimentary rocks.

Materials	Sonic Velocity ft/sec	Transit time μ sec/ft.
Calcite	21053-22000	47.5-45.5
Quartz	18000-18275	55.5-54.7
Sandstones	10000-19600	55.6-51.0
Limestones	21000-23000	47.6-43.5
Dolomites	23000-24000	43.5-42.0
Anhydrite	20000	50.0
Shale	6000-16000	167-62.5
Rock salt	15000	66.7
Water (mud)	5000-5300	200-189
Oil	4300	232
Casing (iron)	17500	57.0

(O. Serra (1984), Schlumberger (1972), & Lynch(1962))

time in the solid and fluid parts of the formation differ approximately by a factor of 4. This tends to be much larger than the individual differences between the variety of solids commonly found in a formation. It is the basis for the formula of Wyllie and others (1956) that expresses the acoustic velocity (V_f) in the formation in terms of the average velocities of the solid (V_s) and fluid (V_w) parts, and the porosity (Φ), which specifies their proportions:

$$1/V_f = \Phi/V_w + (1 - \Phi)/V_s \quad (3)$$

The corresponding formula (Rudman, 1984) for transit time (TT) is

$$TT_f = TT_w \Phi + (1 - \Phi)TT_s \quad (4)$$

Dependence of resistivity on porosity

Electrical resistivity is a measure of the capacity of a substance to transmit electrical current. In most formations electrical current is carried by ions dissolved in the ground water. In brackish water with a sodium chloride concentration above 200 ppm the resistivity will be less than 30 ohm meters, which is much lower than the values given in Table 2 which are typical of the common rock forming silicate and carbonate minerals. Therefore, the principal factors to consider are the resistivity of the ground water and the formation porosity. These factors are combined in the well known formula of Archie (1942):

$$R_f = aR_w \Phi^{-C} \quad (5)$$

where R_f is the formation resistivity, R_w is the ground water resistivity, C is the cementation factor, and a is an empirical constant. Values of C ranging between 2.0 to 3.0 and values of a ranging between 0.6 to 1.0 must be determined experimentally for different geologic settings.

In various studies, Archie's formula has been confirmed for a wide range of porosity, grain size, mineralogy, and texture (Rudman, 1984).

Table 2. Resistivities of common minerals and sediments

Materials	Resistivity (ohm-m)	
	Range	Average
Quartz	$4 \times 10^{10} - 2 \times 10^{14}$	
Anhydrite		10^9
Calcite		2×10^{12}
Rock salt	30 - 10	
Surface waters (sediments)	10 - 100	
Soil waters		100
Natural waters (sediments)	1 - 100	3
Seawater		0.2
Saline waters, 3 percent		0.15
Saline waters, 20 percent		0.05
Consolidated shales	$10 - 8 \times 10^2$	
Sandstones	$1 - 6.4 \times 10$	
Limestones	$50 - 10^7$	
Dolomite	$3.5 - 10^2 - 5 \times 10^3$	
Unconsolidated wet clay		20
Clays	1 - 100	
Alluvium and sands	10 - 800	

(Telford, 1976)

Scale functions

To calculate a pseudosonic log it is necessary to obtain a **scale function** that relates sonic transit time and electrical resistivity. Kim (1964) used the common dependence of transit time and resistivity on porosity to obtain such a scale function. This approach was later elaborated upon by Rudman (1984). Equations 4 and 5 are rearranged to obtain the following expression for porosity:

$$\Phi = (TT_f - TT_s) / (TT_w - TT_s) \quad (6)$$

$$\Phi = (R_f / aR_w)^{-1/C} \quad (7)$$

Then the terms on the right sides of Equations 6 and 7 are equated and rearranged to obtain:

$$TT_f - TT_s = (TT_w - TT_s) a R_w^{1/C} R_f^{-1/C} \quad (8)$$

Finally, the constant terms $A = TT_s$, and $B = (TT_w - TT_s) a R_w^{1/C}$ are substituted to obtain the scale function:

$$TT_f = A + BR_f^{-1/C} \quad (9)$$

According to this function, points representing corresponding values of transit time and resistivity, read from logs recorded in the same test well, should plot close to a curve having the form illustrated in Figure 2. The three empirical constants A, B, and C can be determined from the resistivities and transit times in a set of three points situated on such a curve. The procedure will be described in a later section.

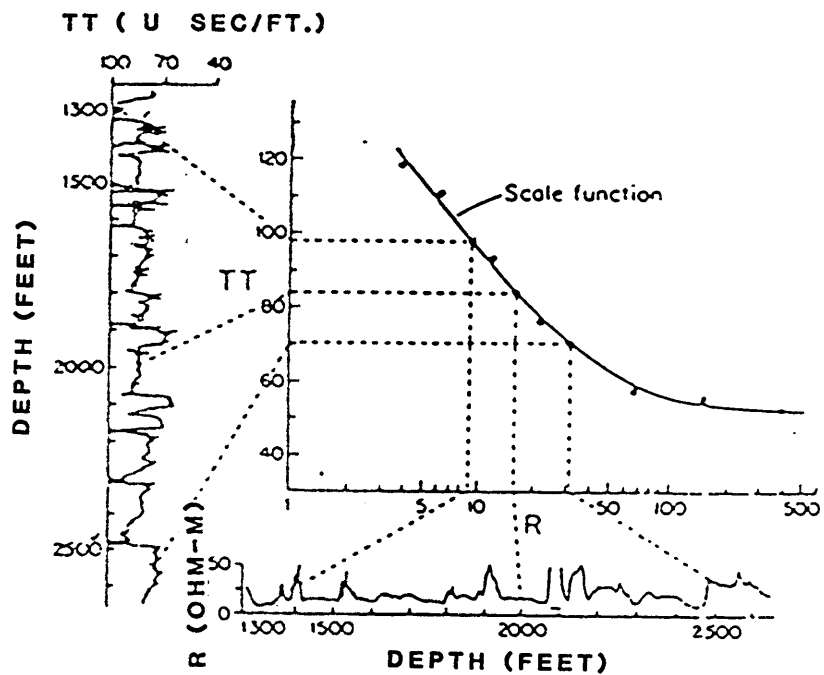


Figure 2. Illustration of a scale function curve: In this sketch resistivity, in ohm-m, and transit time TT, in $\mu\text{s}\cdot\text{ft}$ from a specific depth interval, form a pair of values for each point. (Rudman, 1984 as modified from Kim, 1964).

CONVENTIONAL WELL LOGS

Sonic logs

Sonic logs measure the transit time of a high frequency acoustic wave through a given interval of rock. Figure 3 illustrates the type of sonic device used in this study. The distance from the transmitter to the first receiver is 3 ft., and the distance between the two receivers is typically set at 2 ft. Also pictured in Figure 3 are the ray paths followed by the first acoustic wave arrivals. Since the first arrivals travel in the formation only a few inches or less from the borehole wall, the depth of investigation of the sonic device is small. This is a non-borehole compensated logging device.

Resistivity logs

The typical electrode configurations of conventional unfocused normal log and focused laterolog devices for measuring resistivity are shown in Figure 4. The normal device measures the potential drop between an electrode M situated 16 inches (short normal) or 64 inches (long normal) from a current input electrode A, and a second electrode N situated a large distance, considered infinite, from A.

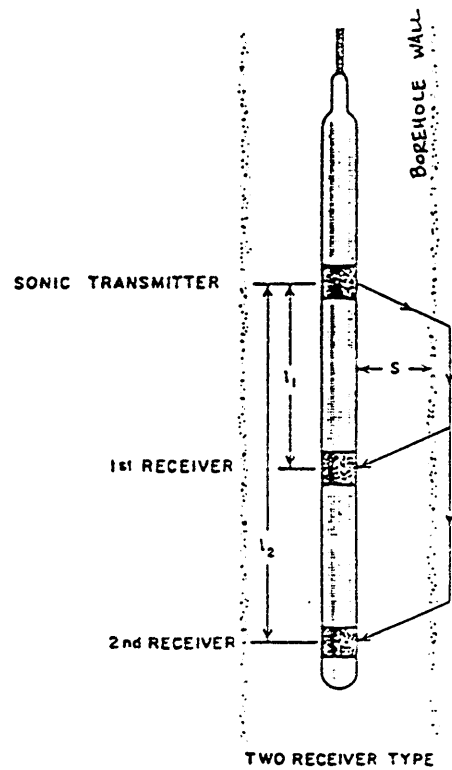


Figure 3. Conventional non-borehole compensated device: Ray paths for the two receiver-one transmitter sonic device. (Lynch, 1962).

In a homogeneous medium the total zone of investigation is a spherical shell centered on A with an inner radius AM and an outer radius taken to be infinite. However, 50 percent of the potential drop occurs within the spherical shell with inner radius AM and outer radius $2 AM$ (Figure 4A). In a non-homogeneous medium consisting of interbedded layers of differing resistivity, electrical current is refracted at layer boundaries. This severely distorts the resistivity measurements for beds thinner than $2 AM$, so that reliable values of R_f can be measured only in thicker layers (Lynch, 1962).

The focused laterlog device consists of a central electrode A_0 from which current I_0 flows into the formation. Two long electrodes A_1 and A_2 , maintained at the same potential as A_0 , are situated above and below. Because there is no potential drop between A_0 and A_1 or A_2 , the current I_0 is focused into a horizontal sheet having a thickness approximately equal to the length of the A_0 electrode. This current, which is recorded, penetrates several feet into the formation as a sheet, and is proportional to the resistivity in the zone of penetration (Figure 4B).

The invaded zone

A feature of deep wells drilled with rotary drills is the annulus of invasion (Figure 5) produced by infiltration of drilling fluid into the formation. Insofar as the resistivity of the filtrate differs from that of the natural formation fluid it displaces, the measured resistivity will differ from the value of R_f in the uncontaminated formation. This difference tends to be larger for laterolog measurements than for normal log measurements in thick beds, because the normal logs test to a greater distance from the borehole. However, in most shallow fresh/brackish water wells invasion is minimal, and the water commonly used as a drilling fluid does not differ substantially from the natural formation water. Therefore, in these wells the laterolog, which is sensitive to thin beds, provides a more detailed and reliable record of variations in formation resistivity than the normal logs.

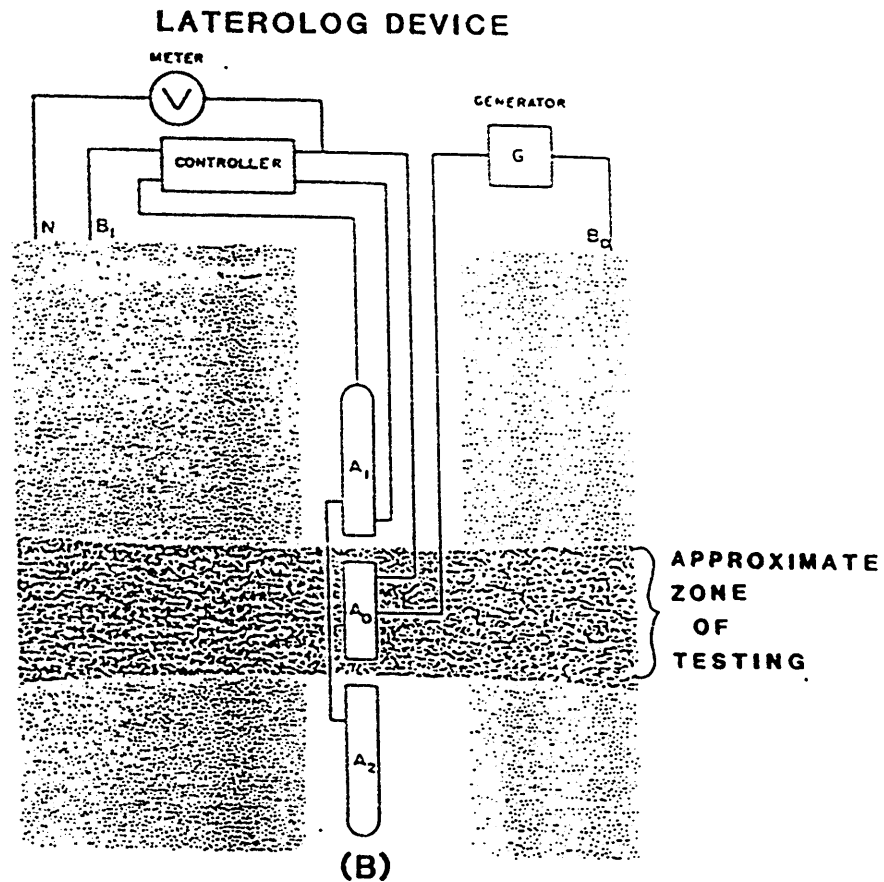
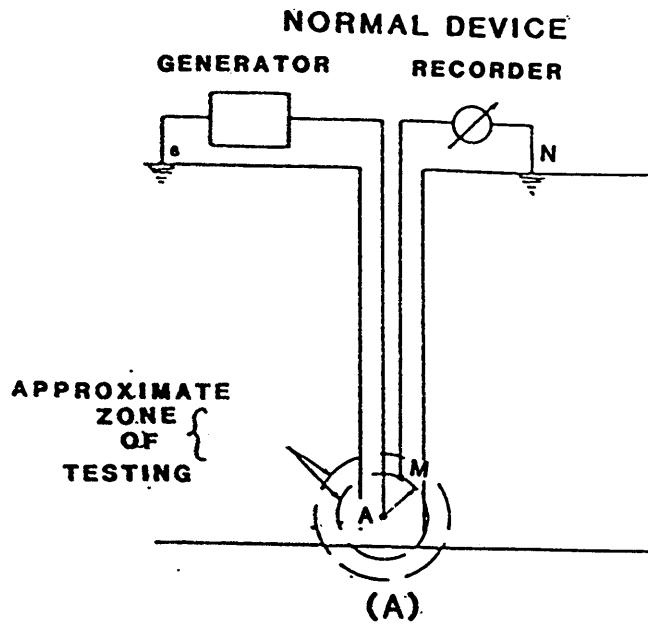


Figure 4. Electrode configurations: for the Normal (A), and Laterlog (B) devices with the zone of testing exhibited in each diagram (Normal and Lateral from Serra, 1984 & Laterolog from Lynch, 1962).

In some deep wells, where invasion is significant, sonic transit times are distorted by the presence of a mudcake (Figure 5) which consists of drilling fluid additives that accumulate during the process of invasion. This source of distortion is usually not present in shallow fresh/brackish water wells.

Smoothing

A scale function (Equation 9) for calculating pseudosonic logs can be determined from an appropriate graph of transit time versus resistivity (Figure 2). Before such a graph is prepared, the sonic and resistivity logs from a test well should be smoothed by a procedure that insures, insofar as possible, that corresponding values represent more or less the same zone in a formation. This is necessary because values of TT and R_r read at the same depth from unsmoothed logs do not represent exactly the same zones owing to differences in sensor spacing and response. Furthermore, the particular sonic logs used in the study display some locally spurious signals caused by cycle skipping as well as the fact that the logging device was not designed to compensate for irregularities in well diameter. To suppress their effects, smoothed logs were prepared by the method of running averages. Values of TT and R_r were obtained at one foot intervals by interpolation between control values read at the peaks and troughs of the analog well logs. Separate smoothed logs were then prepared from 5 point, 10 point, and 20 point running averages.

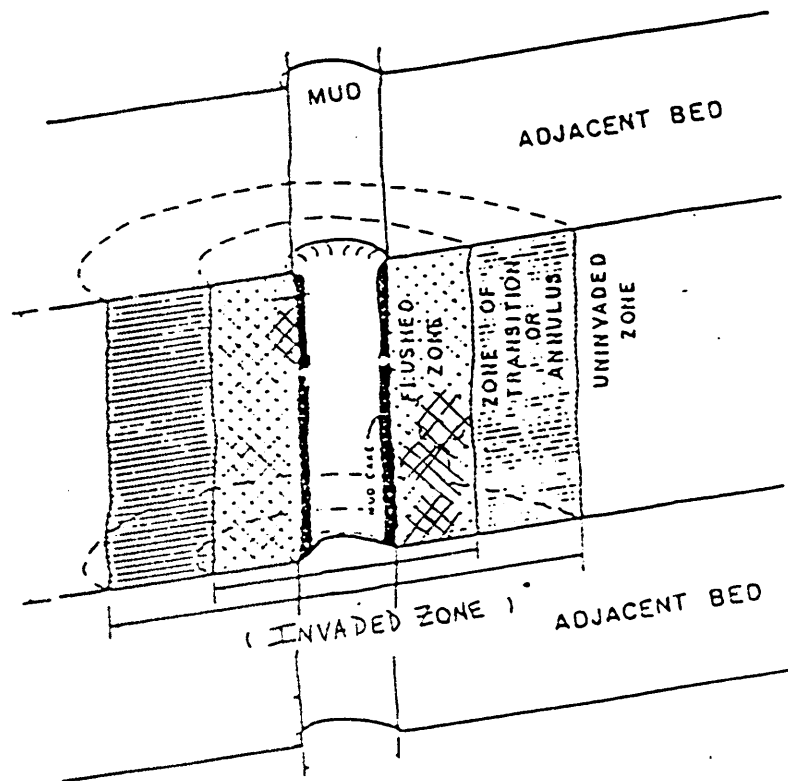
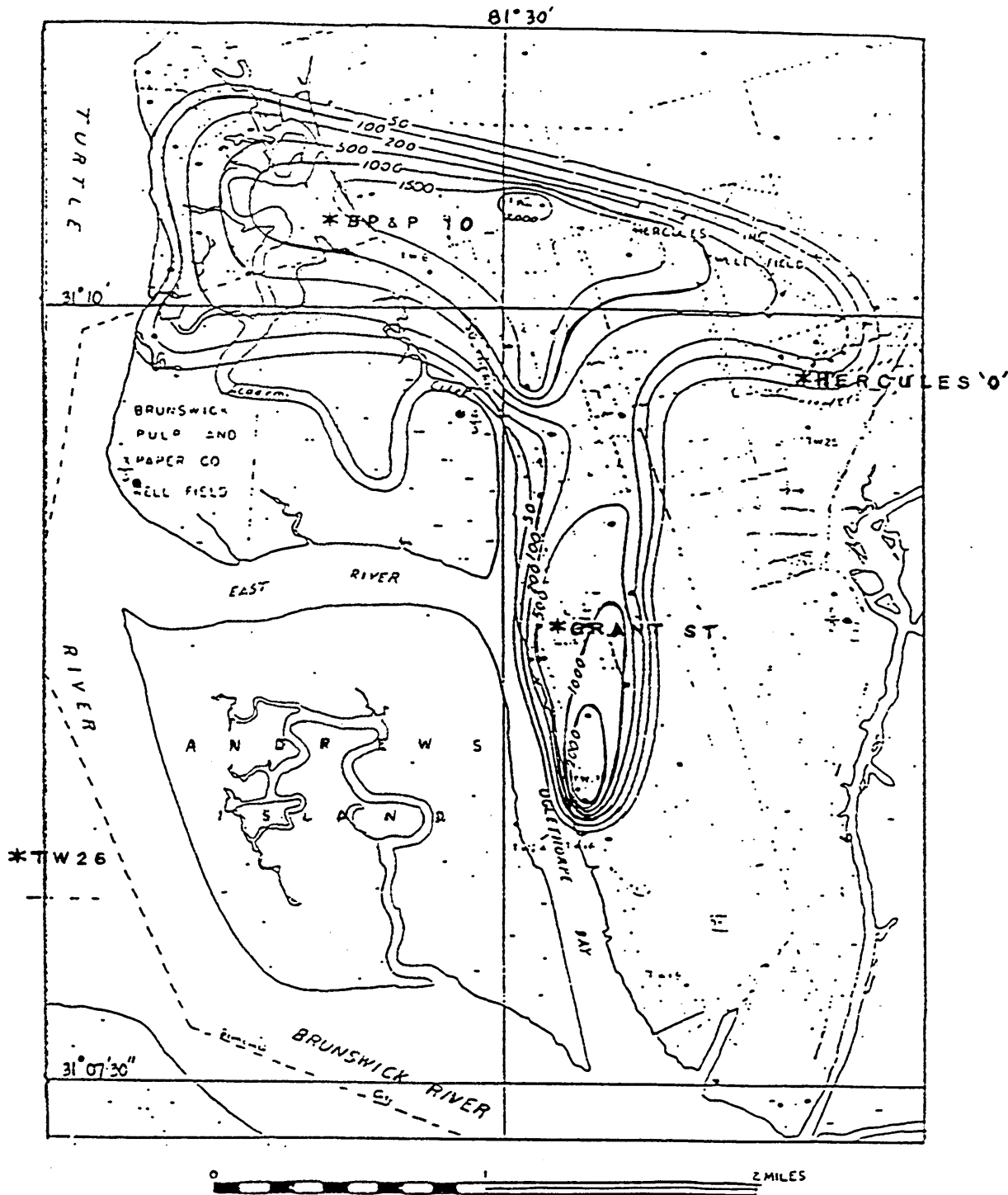


Figure 5. Borehole environment with invaded zone: idealized version of what happens when fluids from the borehole invade the surrounding rock (Asquith, 1982 as obtained from Schlumberger Well Services, 1977.). The invaded zone (borehole, flushed zone, and zone of transition) is cylindrical in nature.

TEST WELLS

Geologic Setting

The four test wells used in this study are located in a well field near Brunswick, Georgia (Figure 6). The basic rock formations range from Holocene to early Eocene in age and consist of a thick sequence (more than 4,000 ft.) of carbonate rocks overlain by 500 - 700 feet of clastic beds, mostly sand, silt, and claystone (Gregg and Zimmerman, 1974). The Ocala Limestone of Oligocene (?) and Eocene age makes up one of the most productive fresh water reservoirs in the U.S., which is called the Floridan aquifer. This aquifer occurs at a depth of 500 ft. and is about 500 ft. thick. At the top, a permeable zone ranges from 86 to 104 ft. in thickness, and a basal permeable zone at a depth of 860 ft. ranges from 16 to 110 ft. in thickness. Because of excessive pumping of the Floridan aquifer resulting in a water level decline, brackish water has migrated upward and is still moving via fractures, faults, and solution enlarged channels from the lower part of the Tertiary carbonate sequence (Gill & Mitchell, 1979) into the aquifer as shown in Figure 6.



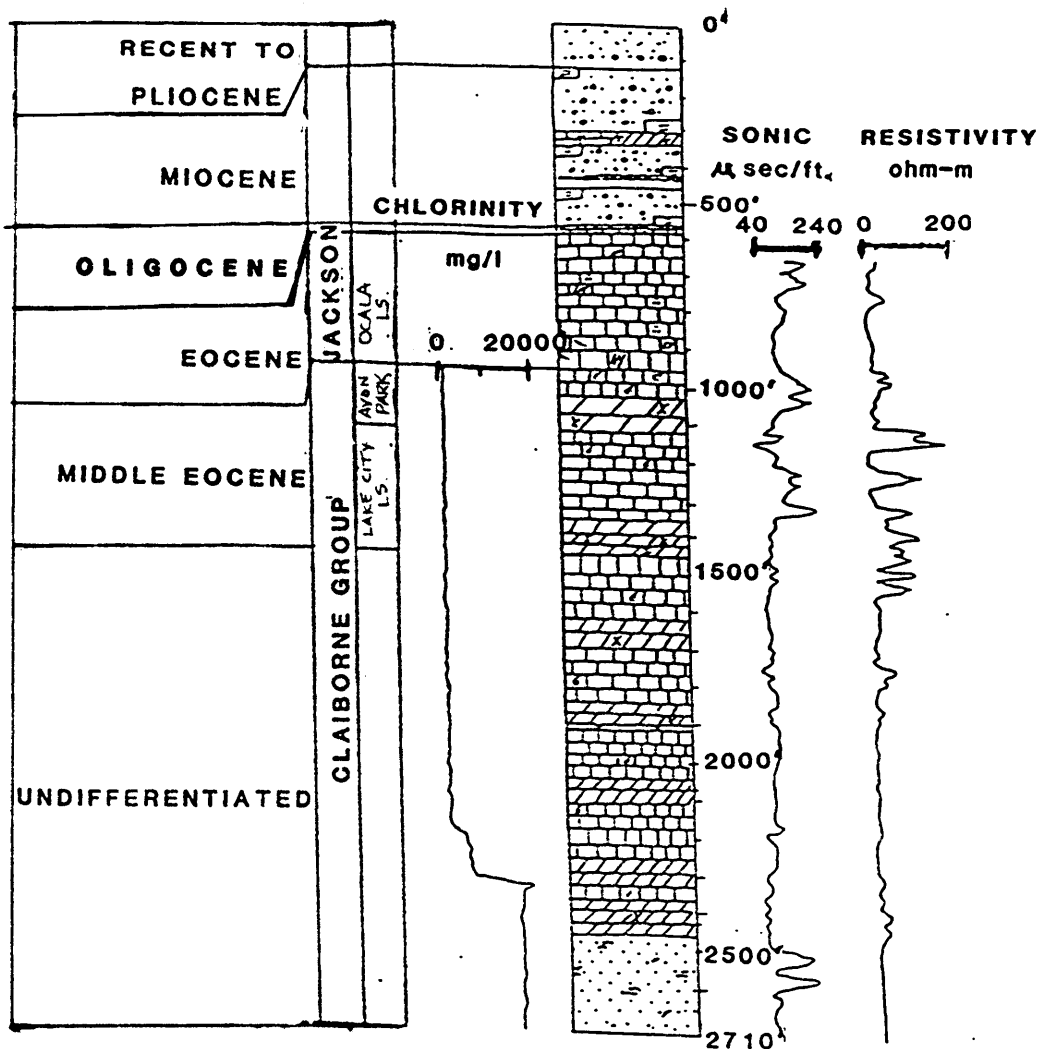
EXPLANATION
 — 1000 — LINE OF EQUAL CHLORIDE CONCENTRATION
 INTERVAL VARIES, IN MILLIGRAMS PER LITER

Figure 6. Map of well field with chloride concentration contours: Pictured in this diagram are the chloride concentrations in the upper water-bearing zone of the Floridan aquifer for October, 1982 along with the location of TW26, Grant St., BP&P 10, and Hercules 'O' in the well field. Chloride concentration values from Stiles and Matthews (1983). (Krauss, et.al., 1984.)


Description of test wells


Locations of the four test wells are shown in Figure 6. Best described is Test Well No. 26 (TW26) which reaches a depth of 2720 feet. A lithologic log prepared from drill cuttings is shown in Figure 7 together with a sonic log, laterolog, and a log of chloride concentration in the well. Because the sonic log was run after casing had been set to a depth of 1520 feet, reliable data is available only for the deeper uncased part of the well. TW26 penetrates mostly limestones and dolomites ranging from Paleocene through Oligocene in age. These rocks are overlain by a terrigenous clastic sequence with minor carbonates that range from Miocene through Pleistocene in age. A focused resistivity log (Figure 7) was run in this shallow section, but a corresponding sonic log was not obtained. Above the depth of 2100 feet the carbonate rocks possess variable intergranular porosity, but below this depth are vugs, caverns, and solution enlarged channels. These openings are the conduits for upward migration of brackish water.

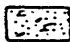
Other test wells include the Grant Street Well (GS) reaching a depth of 980 feet, the BP&P No. 10 Well reaching a depth of 1030 feet, and the Hercules 'O' Well reaching a depth of 865 feet. No detailed stratigraphic logs or drillers' logs are available for these three wells. All four test wells penetrate three phosphate marker beds of Miocene gas which are useful for correlation purposes (Gill, personal communication). Except for local variations the four test wells penetrate basically the same lithologic section as seen in the example presented in Figure 8.

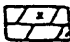


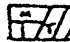
EXPLANATION


- 

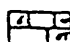
FINE-GRAINED SAND & SILT WITH GRAVEL
- 

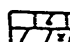
SANDY LIMESTONE
- 


DOLOMITE
- 

APHANITIC TO FINELY CRYSTALLINE DOLOSTONE
- 

MUDSTONE OR SILTSTONE
- 

INTERBEDDED CLAY ZONES AND PHOSPHATE ZONE
- 

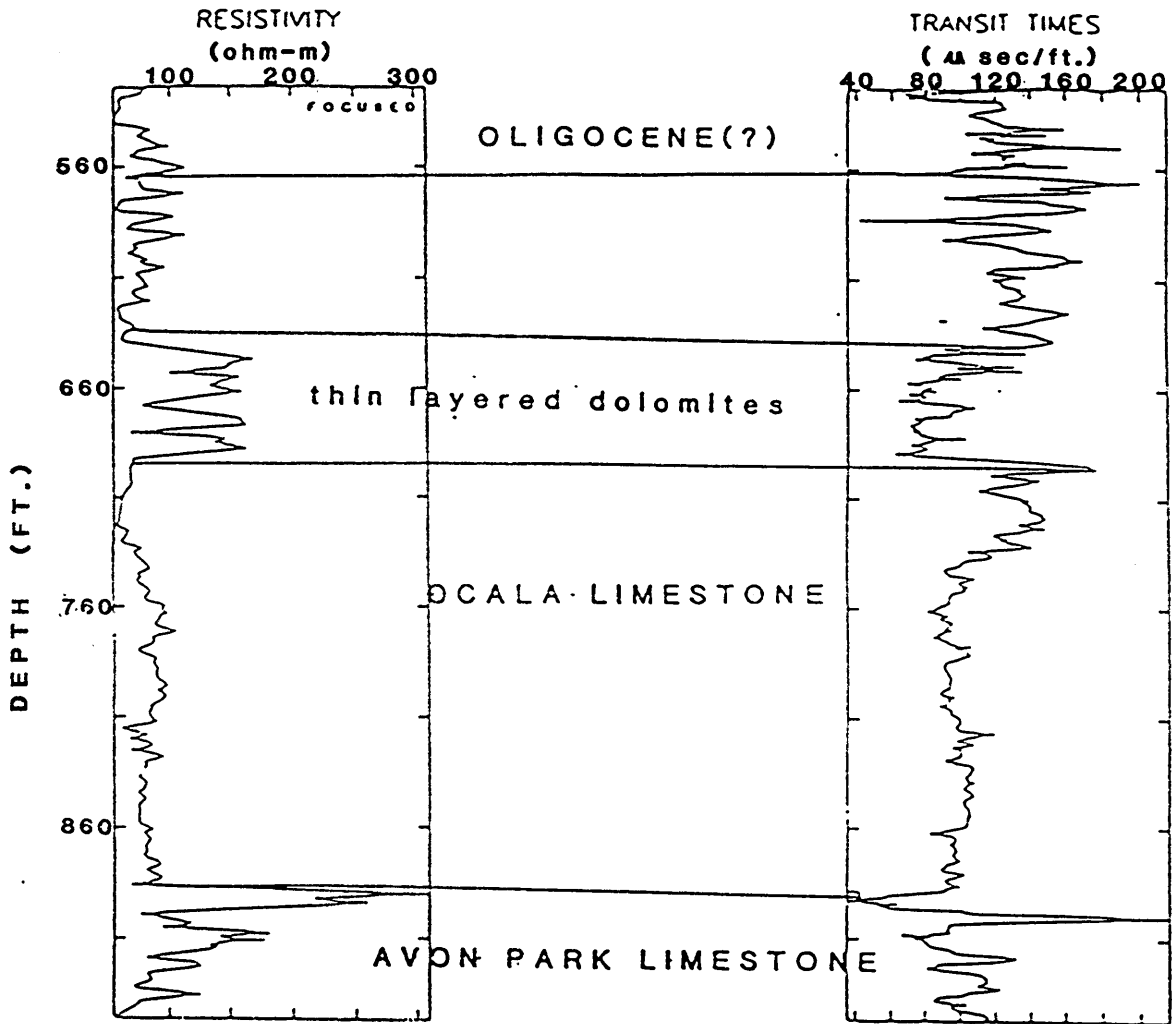
FOSSILIFEROUS LIMESTONE WITH FINE DOLOMITE RHOMBS
- 

FOSSILIFEROUS LS., DOLOMITIC LS., & APHANITIC TO CRYSTALLINE DOLOSTONE
- 

CHERT (BARS)

Figure 7. Generalized stratigraphic column for TW26: Stratigraphic column prepared from geologic log (Gill and Mitchell, 1979) with chlorinity log, non-borehole compensated sonic log, and a laterolog (Georgia Water Resources Division, 1986).

GRANT ST. WELL LOGS



BASE OF OCALA DETERMINED.
FROM WELL LOG CHARACTERISTICS

Figure 8. Plot of Grant St. logs: an example of the general stratigraphy for the Brunswick area (< 1,000 ft) using the focused resistivity and sonic logs from the Grant St. well (Logs from Georgia Water Resource Division, 1986).

PSEUDOSONIC LOGS

Transit time versus resistivity plots

Graphs showing the empirical dependence of transit time on resistivity are needed to determine the scale function for calculating pseudosonic logs. Data for preparing these graphs were obtained from the analog sonic and laterologs from each test well. As described above, the depths and the values of TT_r or R_r read from peaks and troughs of each log were used to interpolate values at one foot intervals. Separate graphs were prepared by plotting these interpolated values, and by plotting 5 point, 10 point, and 20 point running averages of these values.

Graphs for TW26 are presented in Figure 9. Unlike the results of Rudman (1984) that are reproduced in Figure 2, these points do not group close to a single curve representing the scale function. Although the large scatter may be caused partly by real geologic effects, the marginal quality of sections of the logs available for the study may be a factor. Despite this large scatter, close inspection of the graphs reveals that the points are distributed in three general groupings. This suggests that different scale functions describe the relationship between transit time and resistivity in different parts of the well.

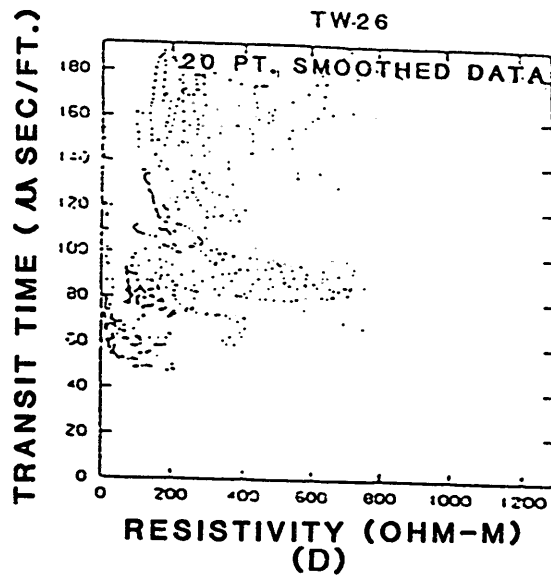
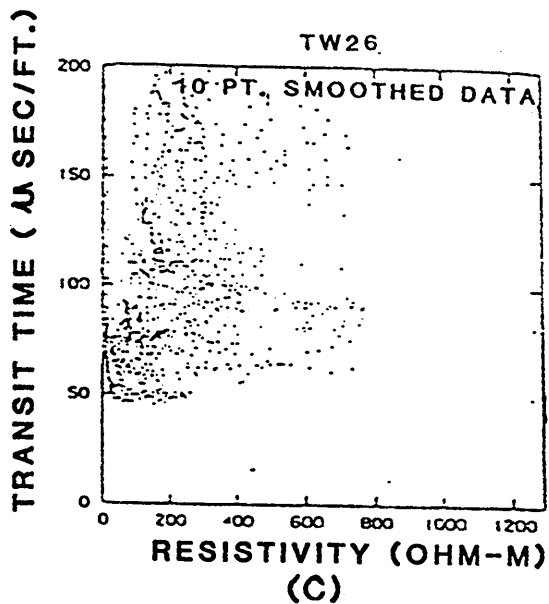
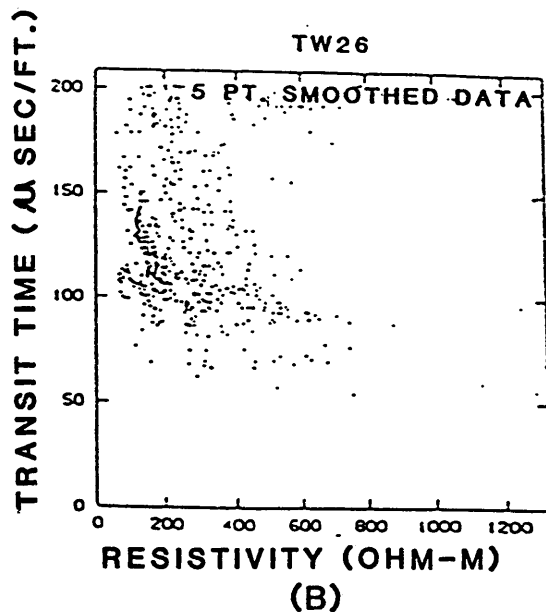
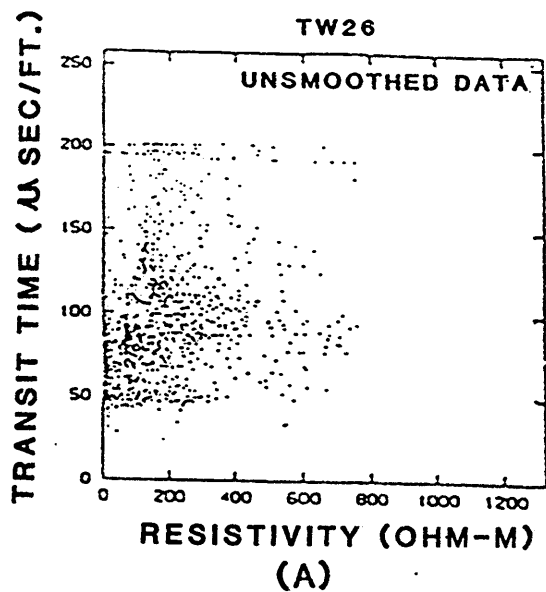
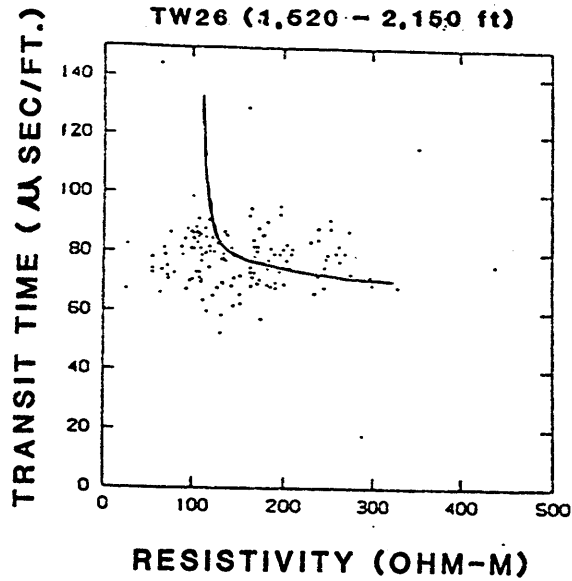
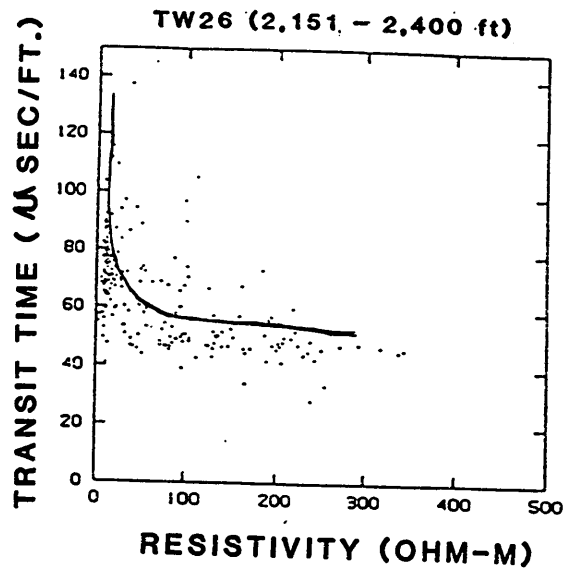


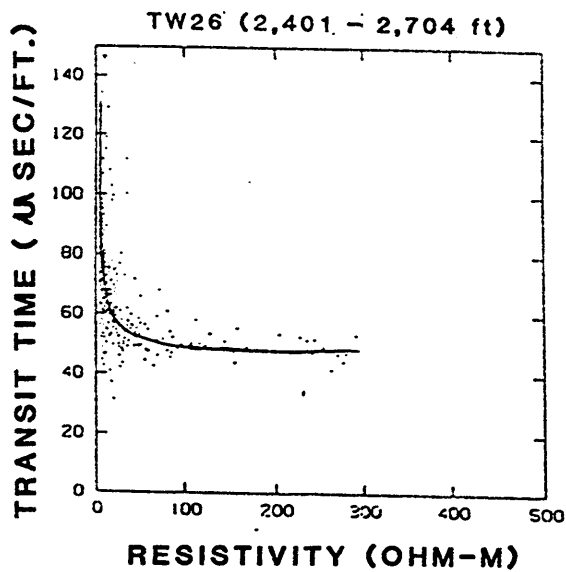
Figure 9. TT vs. R plots: Plots for TW26 (1,520 - 2,717 ft.) include (A) values interpolated at 1 foot intervals from logs, (B) values of 5 point running averages, (C) 10 point running averages, and (D) 20 point running averages calculated from values interpolated at 1 foot intervals.



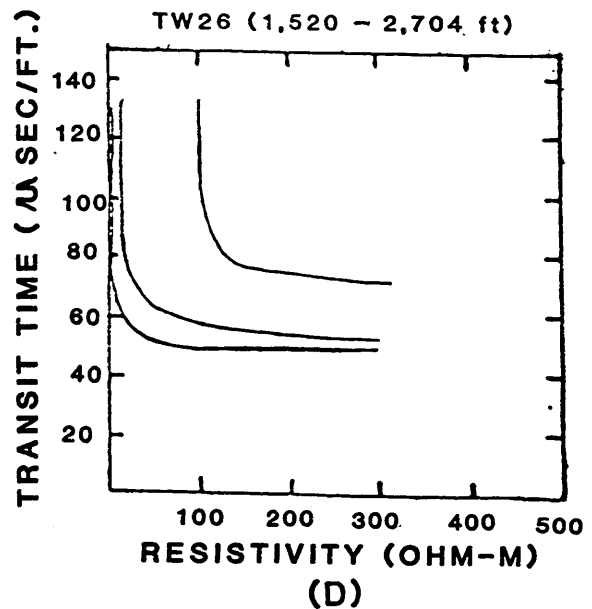
(A)



(B)



(C)



(D)

Figure 10. TT vs. R plots for TW26: plots from 20 pt. running averages for the depth intervals of (A) 1520 - 2150 ft., (B) 2151 - 2400 ft., and (C) 2401 - 2704 ft. (D) A comparison of curves drawn through these groups of points.

A factor which could contribute to the distributions seen in Figure 9 is the salinity of the formation water. The chlorinity log for this well (Figure 7) indicates that distinct changes in the chloride concentration occur at depths of 2150 feet and 2400 feet.

To test this supposition three separate graphs were plotted using data from 1) the interval above 2150 feet, 2) the interval from 2150 feet to 2400 feet, and 3) the interval below 2400 feet. The results in Figure 10 indicate that points from these different intervals tend to plot in different zones of the graph, confirming the idea that the scale function is influenced by salinity as well as porosity. Although porosity is the dominant factor, the distribution of points in these three zones is consistent with the fact that increasing salinity can significantly reduce resistivity while not appreciably affecting transit time.

Graphs of transit time versus resistivity for the other three test wells are shown in Figure 11. Multiple groupings of points similar to those seen in TW26 are not seen in the Grant St. and the Hercules 'O' wells but the graphs indicate a different scale function for each well. Data from the BP&P No. 10 well reveal two separate groupings. The grouping with lower resistivity values consists of data from the upper and lower intervals of 557 - 767 feet and 869 - 1024 feet, and the grouping with higher resistivity includes data from the intermediate interval of 768 - 868 feet. The differences in resistivity suggest higher salinity in the upper and lower intervals which include the permeable zones of the Floridan aquifer. Higher resistivity in the intermediate interval indicates lower salinity in this more impermeable interval. Although chlorinity logs are not available for these wells, the average chloride concentration in the upper water bearing zone of the Floridan aquifer at these well sites can be estimated from Figure 6. Estimates of 75 ppm for the Hercules 'O' Well, 750 ppm for the Grant St. Well, and 1400 ppm for the BP&P No. 10 Well confirm that the different groupings on the graphs in Figure 11 are influenced by salinity.

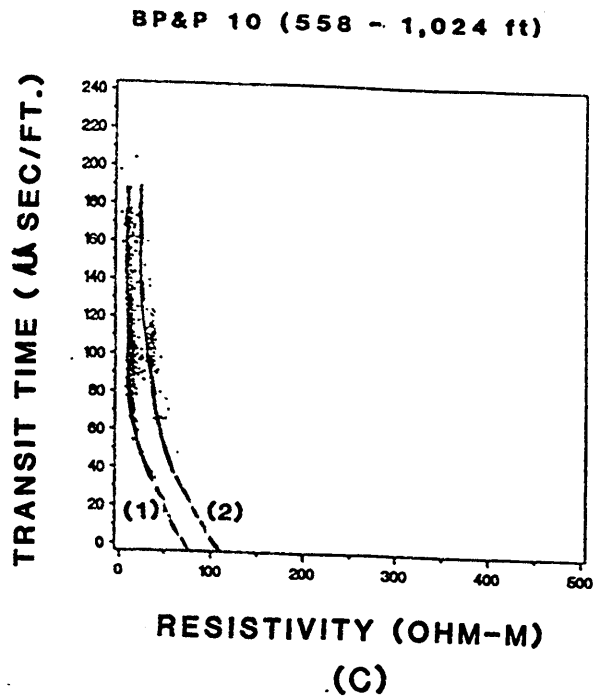
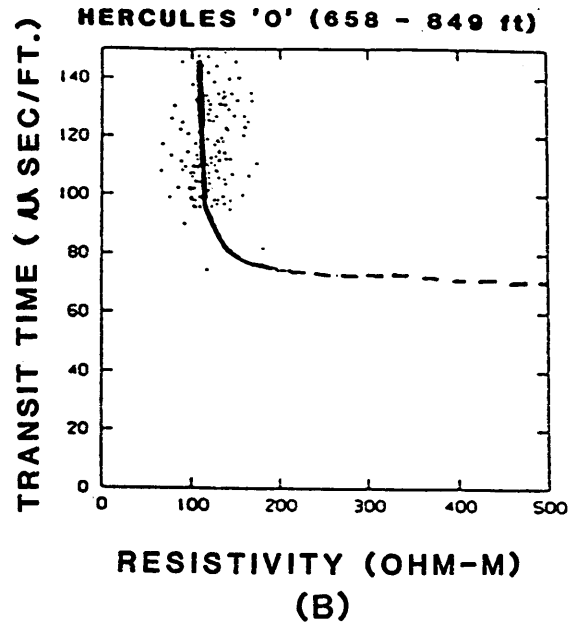
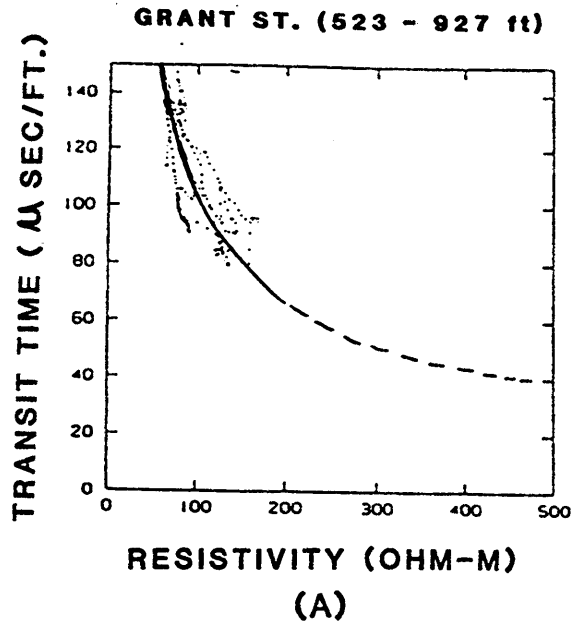


Figure 11. TT vs. R plots: Values of 20 pt. running averages from Grant St., BP&P No. 10, and Hercules 'O' wells.

Scale functions

Scale functions were prepared by arbitrarily fitting curves to the points plotted in Figure 10 and Figure 11. Consider first the data from 1520 feet to 2150 feet in TW26 (Figure 10A), from 658 ft. to 849 ft. in the Hercules 'O' Well (Figure 11C), and from 523 ft. to 927 ft. in the Grant St. Well (Figure 11A). All of these intervals penetrate carbonate rocks with essentially fresh formation water, the chloride concentration being less than 800 ppm. The same scale function curve was fitted to both the Hercules 'O' and the Grant St. intervals with a slightly different one applied to the shallow interval in TW26.

An average scale function, which combines the characteristics of the high porosity rocks encountered in the Hercules 'O' and Grant St. Wells with the generally lower porosity rocks from the shallow interval in TW26 could be calculated from all three wells. Porosity estimates for these rocks were made from borehole televiewer images (Gill, personal communication). The result would be a scale function for carbonate rocks containing fresh formation water that should be generally applicable over a wide range of porosities. Even though there is some variability in the porosities, which are mainly intergranular, from these three intervals, they still differ from the vuggy, cavernous, and solution-enlarged channel porosity found in the other intervals in TW26 and the BP&P 10 Well.

Consider next the data from 2401 ft. to 2704 ft. in TW26 (Figure 10C). Here the salinity of the formation water is close to that of standard sea water (chlorinity approximately 19,000 ppm, salinity approximately 35,000 ppm). This section consists of carbonate rocks with fractures, cavities, and intergranular pores. Borehole televiewer images and lithologic descriptions of TW26 indicate a porosity range that is somewhat higher than what was encountered in the sections containing fresh formation water (Gill, personal communication). The scale function in Figure 10C, then, should be generally applicable for carbonate rocks containing saline formation water that is similar to sea water.

The intervals in TW26 from 2150 to 2400 ft. (Figure 10B) and in BP&P No. 10 from 557 to 1024 ft. (Figure 11C) penetrate carbonate rocks containing brackish formation water in which the chlorinity is in the range of 1400 - 7500 ppm. The porosity range is similar to that encountered in the section containing saline formation water (Gill, personal communication). The scale function fitted to the points in Figure 10B is intermediate to the functions seen in Figures 10A and 10C. The scale functions are plotted together in Figure 10D.

Each of these three scale function curves corresponds to a section of carbonate rock in which the salinity of the formation fluid is more or less uniform. These curves are offset from one another in a way that is consistent with the fact that similarly porous zones with increasing salinity of the formation fluid can act to reduce the electrical resistivity and possibly the sonic transit time. As noted earlier, scale functions for the Grant Street, Hercules 'O' and BP&P No. 10 Wells, fitted to the data in Figure 11A, Figure 11B, and Figure 11C, are consistent with this pattern. Although average chlorinity values in these wells can be estimated from Figure 6, the extent to which significant chlorinity gradients may exist has not been measured.

For each of the scale function curves illustrated in Figure 10D, the constants A, B, and C in Equation 8 were calculated by the method presented by Rudman (1984). A multiplication constant Q is chosen arbitrarily, then three points at coordinates (R_{f1}, TT_{f1}) , (R_{f2}, TT_{f2}) , and (R_{f3}, TT_{f3}) are located on the curve so that $R_{f2} = QR_{f1}$, and $R_{f3} = QR_{f2}$. The value of Q should be chosen to insure that these points are well distributed along the entire curve. The coordinates are then substituted into Equation 8 to obtain three separate equations in A, B, and C. Combining them and rearranging yields:

$$C = \log Q / \log[(TT_{f1} - TT_{f2}) / (TT_{f2} - TT_{f3})] \quad (10)$$

$$B = (TT_{f1} - TT_{f2}) / (R_{f1}^{-1/C} - R_{f2}^{-1/C}) \quad (11)$$

$$A = TT_{f1} - BR_{f1}^{-1/C} \quad (12)$$

Values of A, B, and C for each of the scale functions are presented in Table 3. It should be noted that Equation 11 is the correct form of the equation originally presented by Rudman (1984, Equation 34) which is incorrect.

The three scale function curves correspond to geologic sections that are lithologically similar, but differ in the chlorinity, and therefore, the salinity of the formation water. Therefore, the possibility exists for determining a single scale function with chlorinity or salinity dependent coefficients. The following method was used to accomplish this. From the three curves in Figure 10D three values were obtained together with corresponding chlorinity values for each of the coefficients A, B, and C. These data are sufficient to express each coefficient by a quadratic function of chlorinity. The following results were obtained:

$$A = 2.04 \times 10^{-7} Cl^2 - 5.22 \times 10^{-3} Cl + 70.9 \quad (13)$$

$$B = 1.59 \times 10^6 Cl^2 - 4.13 \times 10^{10} Cl + 2.11 \times 10^{14} \quad (14)$$

$$C = -6.32 \times 10^{-9} Cl^2 + 1.56 \times 10^{-4} Cl + 0.114 \quad (15)$$

Substitution of these results into Equation 8 yields an expression for sonic transit time in terms of the electrical resistivity of the formation and the chlorinity (Cl), expressed in ppm, of the formation fluid. The data available for this study were insufficient to ascertain if a mathematical function different from the quadratic function might be more appropriate for representing the chlorinity dependence of A, B, and C. It is important to note that these results are based entirely upon data from carbonate rocks.

Sonic logs were not available for intervals in the test wells penetrating clastic sections of interbedded sand and claystone. The resistivity log in this interval of TW26, where the formation water is fresh, recorded a different range of resistivity values than was found for the carbonate section containing fresh formation water. This indicates that the scale function for the clastic sand/clay section must

Table 3. Values of A, B, and C for each of the scale function in the TW26, Hercules 'O', Grant St., and BP&P No. 10 Wells

Wells	A	B	C
TW26 (1520 - 2150 ft.)	66.9	7666.3	0.75
Hercules 'O' (658 - 899 ft.)	54.8	7836.3	0.94
Grant St. (523 - 927 ft.)	54.8	7836.3	0.94
TW26 (2151 - 2400 ft.)	45.0	450.0	1.0
BP&P No. 10 (557 - 767 ft.) (869 - 1024 ft.)	10.0	5597.0	0.585
BP&P No. 10 (768 - 868 ft.)	-321.0	1753.0	2.49
TW26 (2401 - 2704 ft.)	43.5	411.4	0.89

be different than the scale function for carbonate rocks. Therefore, data available for this study is restricted to pseudosonic log calculations for the carbonate sections.

Pseudosonic logs for the test wells

Pseudosonic logs were calculated for the test wells using the appropriate scale functions. They are compared with the measured sonic logs in Figures 12 - 15. Judgements about the reliability of these pseudosonic logs are based upon (1) qualitative visual correlation with measured sonic logs and (2) calculation of correlation coefficients.

Sonic and pseudosonic logs from each well were divided into 100 foot sections for visual comparison (Appendix A). Comparison of the pseudosonic and sonic logs for TW26 reveals large variations in quality, ranging from fairly good duplications of detailed features along some portions to less favorable duplication along other portions such as from 1920 ft. to 2030 ft. This deterioration for TW26 is exhibited by a greater difference between the logs in the magnitude of some peaks and troughs.

Figure 12 (2400 - 2510 ft.) is an example from TW26 of a very good visual correlation. The only real difference between the sonic and pseudosonic logs for this section is that the sonic log exhibits more detail. This section as well as the others required a shift of about 1 foot by the pseudosonic log with respect to the sonic log. A possible reason for the shift could be an offset in the reference points used in plotting resistivity and transit time values on the original logs. Appendix A contains the complete sonic and pseudosonic logs for TW26.

Examples of pseudosonic logs and sonic logs from the other three wells are pictured in Figures 13 - Figure 15. The best visual comparison between the pseudosonic and sonic of the Grant St. well occurred between 610 and 720 ft. (Figure 13). As can be seen, there is good correlation between all major peaks and troughs with some mismatching on some of the smaller peaks and troughs.

TW26

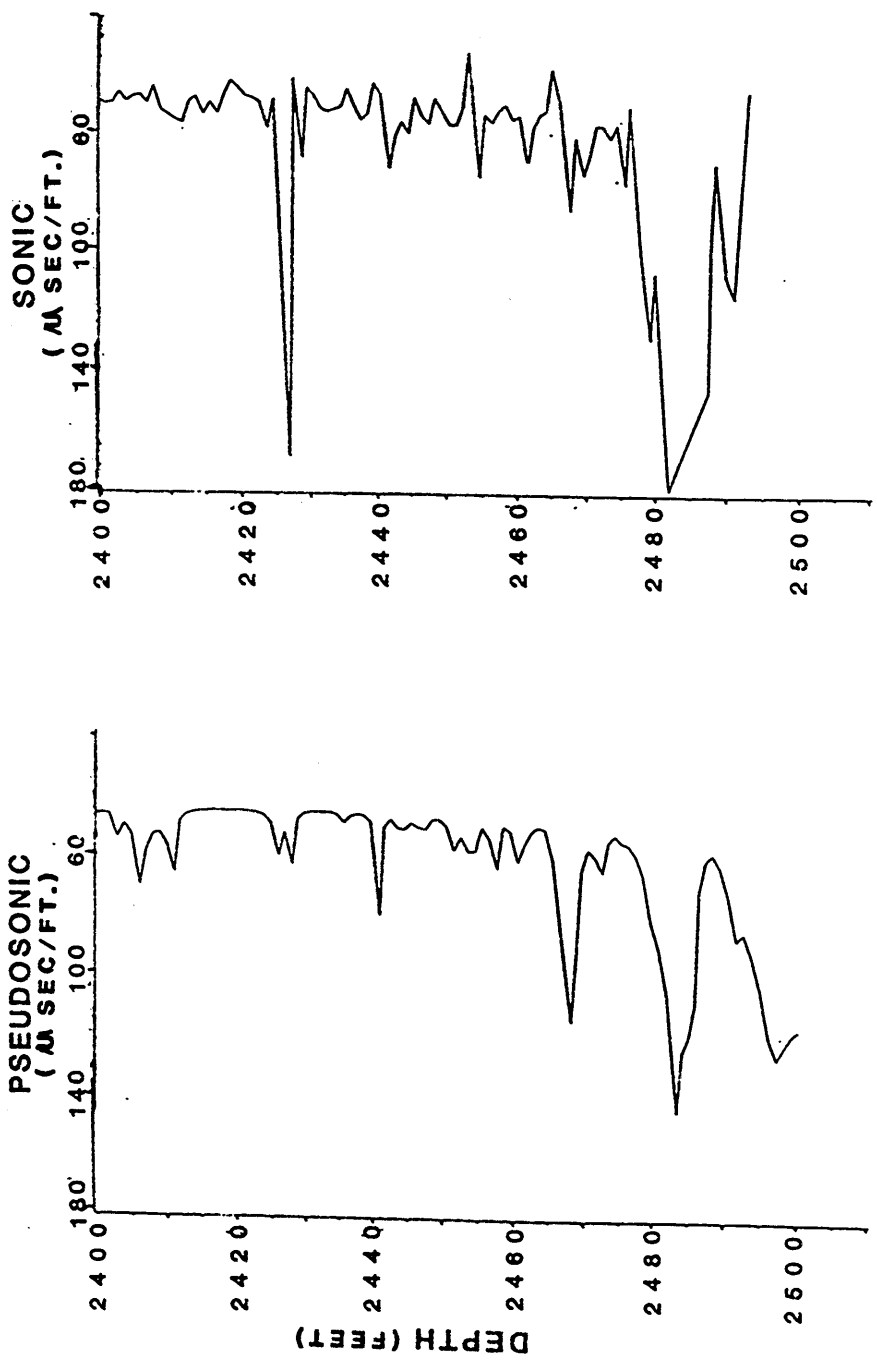


Figure 12. Sonic vs. Pseudosonic (TW26): An example of the visual correlation that exists between the sonic (A) and pseudosonic (B) for a portion of TW26. This particular portion of TW26 (2,400 - 2,510 ft.) exhibits the best correlation for the entire well.

In other sections of the Grant St. well the general trends match fairly well without shifting; however, there are some significant magnitude differences between the pseudosonic and sonic logs (Appendix A).

The best correlation in the Hercules 'O' well occurs in the middle of the log from 640 to 750 ft. The pseudosonic and sonic logs appear similar in form but the magnitudes are somewhat different (Figure 14). The generally poor comparison between the entire sonic and pseudosonic logs for the Hercules 'O' well could be attributed to the overall poor quality of the original sonic log. It along with the resistivity in the shallower portion of the Hercules 'O' well show extreme variability in their values.

In the BP&P No. 10 Well portions of the pseudosonic log for the intervals of 557 - 767 feet and 869 - 1024 feet were calculated using the same scale function, but a different scale function was used to calculate the pseudosonic log for the interval of 768- 868 feet. Although no salinity or chlorinity logs are available from this well, it appears from higher resistivity values in the intermediate interval that here the salinity is lower than in the intervals above and below. This suggests that contamination by brackish water may not have resulted from vertical infiltration from below. Details of the sonic log in the intermediate interval appear to be duplicated better on the pseudosonic log than details in the intervals above and below. This better duplication may be the result of less variation in salinity. Without a chlorinity log, it is not possible to take into account the effects of variations in water chemistry within each of these intervals.

The pseudosonic logs calculated for each well were evaluated numerically by means of a simple cross correlation, Pearson's r, using the equation:

$$r = \frac{\sum_i (x_i - \bar{x})(y_i - \bar{y})}{\sqrt{\sum_i (x_i - \bar{x})^2} \sqrt{\sum_i (y_i - \bar{y})^2}} \quad (16)$$

GRANT ST.

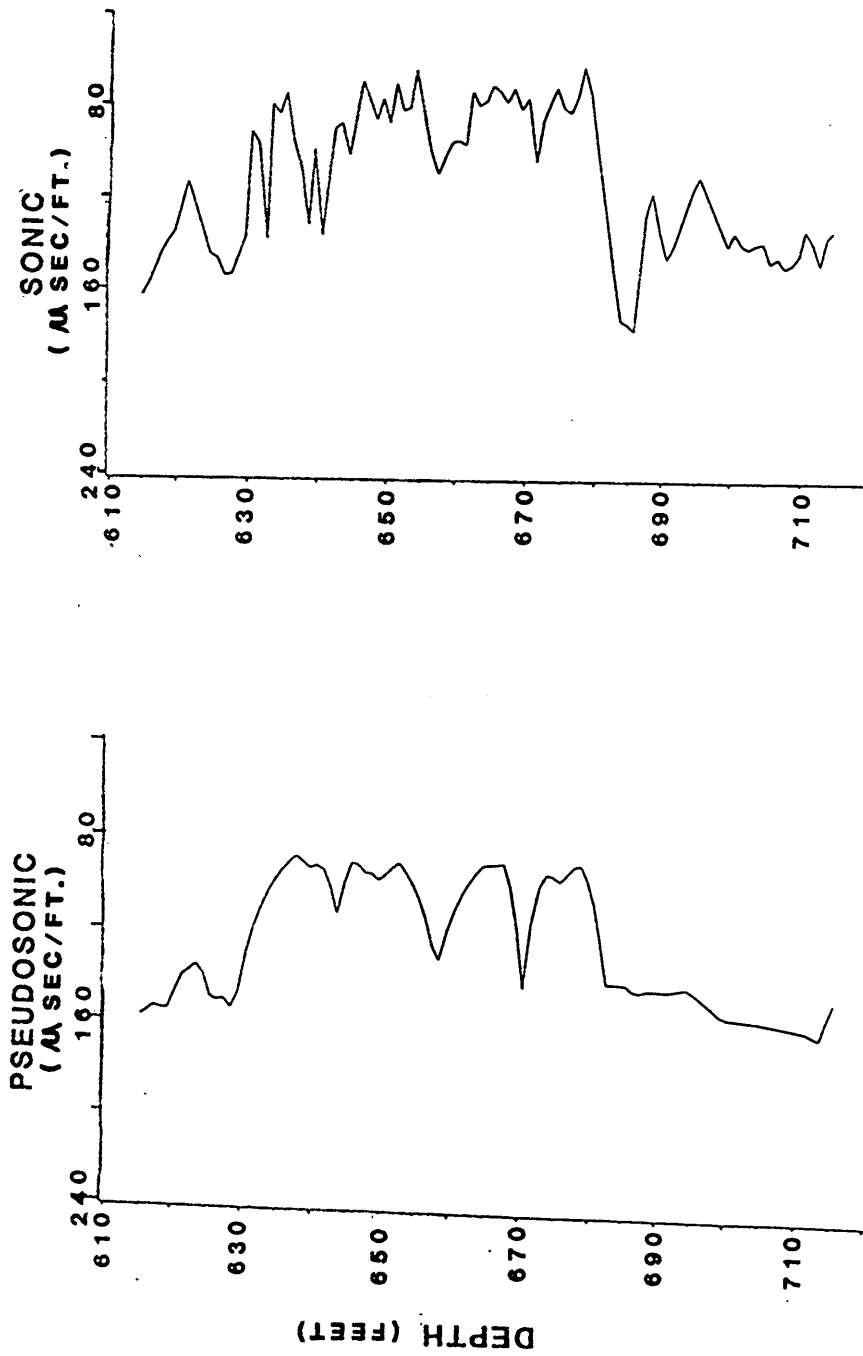


Figure 13. Sonic vs. Pseudosonic (Grant St.): An example of the visual correlation that exists between the sonic (A) and pseudosonic (B) for a portion of the Grant St. well (615 ft. - 715 ft.).

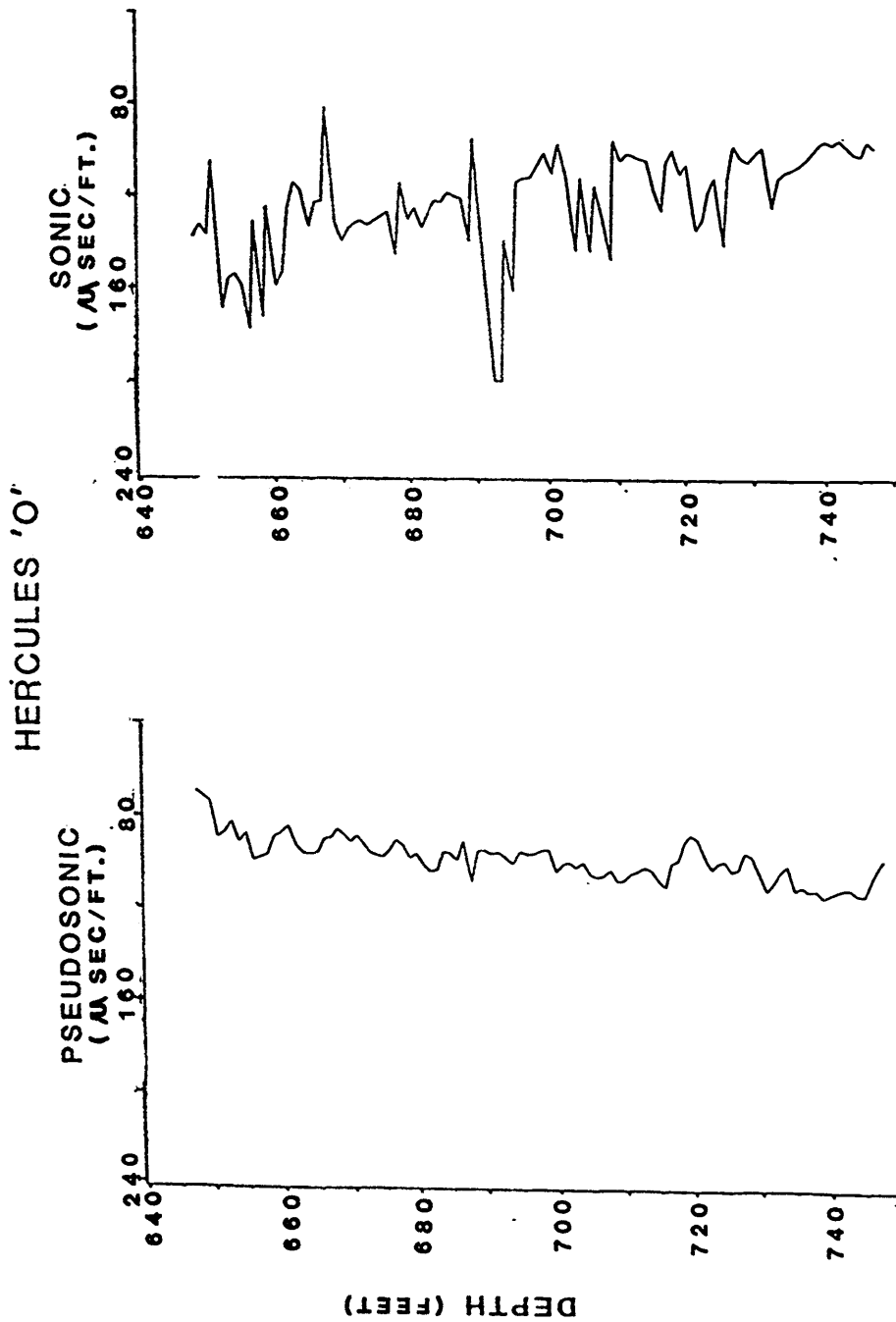
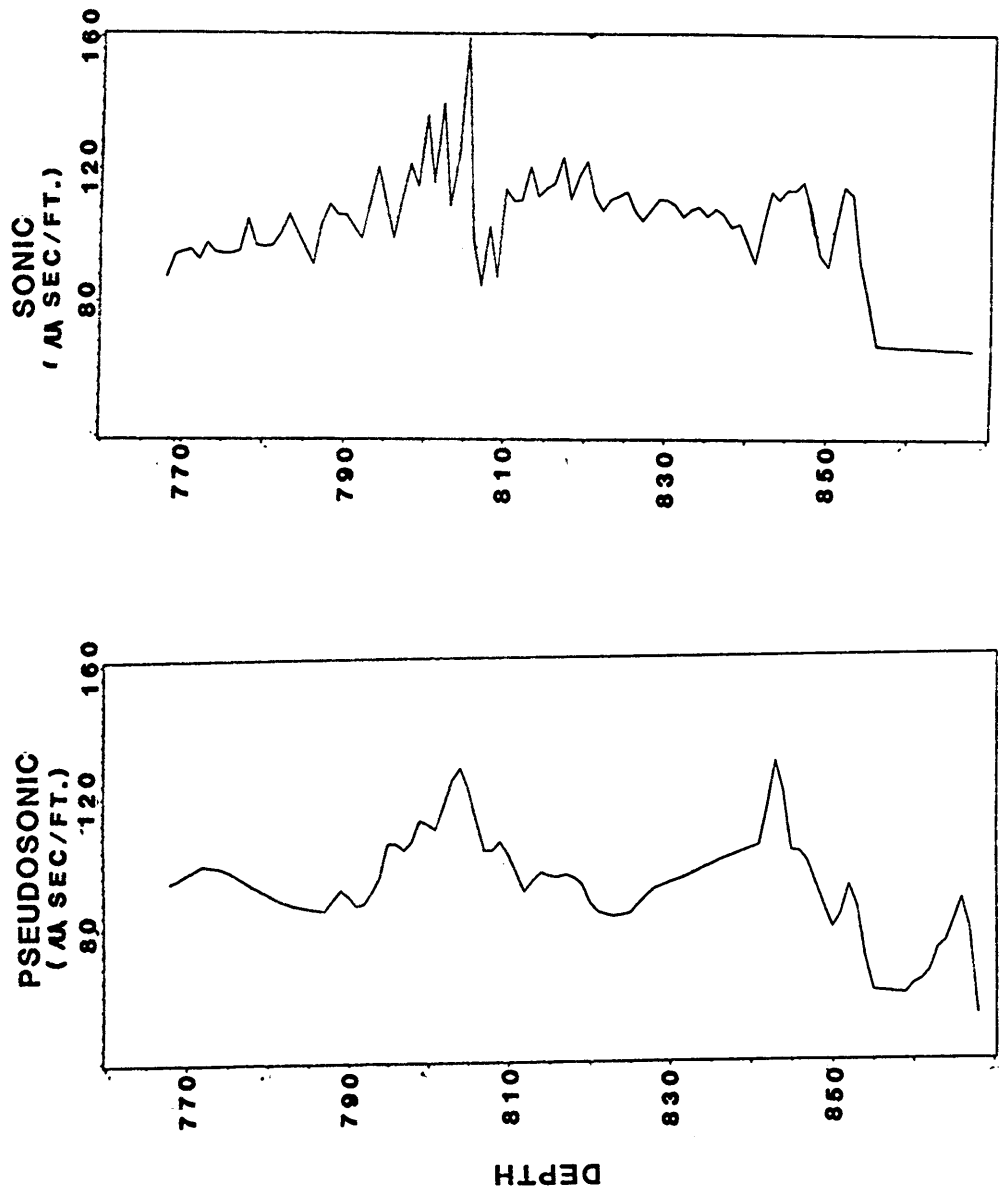


Figure 14. Sonic vs. Pseudosonic (Hercules 'O'): An example of the visual correlation that exists between the sonic (A) and pseudosonic (B) for a portion of the Hercules 'O' well (640 ft. - 750 ft.).

BP&P NO. 10



PSEUDOSONIC LOGS

Figure 15. Sonic vs. Pseudosonic (BP&P 10): An example of the visual correlation that exists between the sonic (A) and the pseudosonic (B) for a portion of the BP&P No. 10 well (750 ft. - 870 ft.).

where r is the correlation coefficient at zero lag and x_i and y_i are the actual and pseudotransit times respectively for i measurements in each well, and \bar{x} and \bar{y} are the average values of the actual and pseudo- transit times in each well. When normalized, a cross-correlation of 1 indicates a perfect match and values near zero indicate very little correlation. The results of the correlation test for the four test wells are listed in Table 4. Figures 12 - 15 as well as being the best visual correlations for each well, also have the highest correlation coefficient among all the intervals for each well. From this quantitative evaluation, considerable differences in the quality of the pseudosonic logs is indicated for different sections in each of the four wells. Because brackish water is actively infiltrating the Floridan Aquifer in this area, significant variations in salinity can be expected. These variations, which cannot be accounted for without chlorinity logs, probably are errors that act to reduce the correlation coefficients.

Table 4. Correlation coefficients or Pearson's r at zero lag for all four test wells.

Wells	Depth Range (ft)	Correlation Coefficients
TW26	1520 - 1620	0.0279970
	1620 - 1720	0.0282000
	1720 - 1820	0.6822342
	1820 - 1920	0.6436211
	1920 - 2020	0.0006184
	2020 - 2150	0.2276723
	2150 - 2250	0.4733780
	2250 - 2350	0.3886307
	2350 - 2400	0.2798760
	2400 - 2510	0.8270534
2510 - 2610	0.7977026	
2610 - 2710	0.6129642	
Grant St.	510 - 610	0.2198379
	610 - 710	0.8281616
	710 - 810	0.7322568
	810 - 940	0.5315630
Hercules "O"	540 - 640	0.2489934
	640 - 740	0.3818367
	740 - 860	0.0860466
BP&P10	557 - 657	0.4447866
	657 - 767	0.4888806
	768 - 868	0.6870785
	869 - 969	0.1559533
	970 - 1024	-0.2082361

SUMMARY AND CONCLUSIONS

Because of the usefulness of sonic logs in formation evaluation, efforts have been made to develop a method for calculating pseudosonic logs for wells in which sonic logs were not originally obtained. By establishing empirical relationships between sonic transit time and electrical resistivity, these efforts attempt to use electrical resistivity in the calculation of pseudosonic logs. In previous studies, a method for accomplishing the conversion has been applied using electrical logs from deep oil and gas wells (Rudman, 1984). Except for the rare concentrations of oil and natural gas, saline water is the formation fluid encountered in these wells. The purpose of the present study is to examine ways of applying this method in relatively shallow wells where the principal formation fluid is fresh or brackish water. The study makes use of data from four wells situated in Brunswick, Georgia. These data include unfocused and focused electrical resistivity logs, non-borehole compensated sonic logs, stratigraphy determined from drill cuttings, measurements of water chemistry, and borehole televiewer images.

It is evident from the data used in this study that the quality of a pseudosonic log is influenced by the particular kind of electrical log used for the conversion. Conventional sonic logs with transmitter and receiver intervals of 2 ft. are sensitive to beds as thin as two feet, but test the formation only in a zone very close to the well. Conventional unfocused electrical resistivity logs are influenced by a much larger zone, and their response to thin beds is significantly distorted by effects of

electrical refraction. Because of this distortion and insensitivity to thin beds, it is impossible to reproduce the detail observed on a sonic log by conversion of a conventional unfocused resistivity log to a pseudosonic log.

Conventional focused electrical resistivity logs are sensitive to beds as thin as one foot, and can provide detail comparable with that seen on sonic logs. However, the measured values of resistivity can differ significantly from natural formation resistivity because of invasion of drilling fluid. In deep oil and gas wells where invasion is variable and may penetrate far into the formation the reliability of pseudosonic logs based on focused resistivity logs can be questionable. In shallow wells invasion is usually much less, and the water used for drilling fluid has electrical resistivities much closer to those of formation water. In these wells focused resistivity logs should produce more detailed and accurate pseudosonic logs. The limited data used in this study confirm this proposition.

The procedure for finding an empirical relationship between sonic transit time and resistivity requires sonic and resistivity logs from a representative well. Values of transit time and resistivity read from corresponding depths on these logs are plotted, and a scale function can then be determined from a curve fitted to the distribution of points. Points on the graphs obtained in this study display considerably more scatter than previously published graphs based upon deep well data (Rudman, 1984). This greater scatter appears to be attributable at least partly to the quality of the available logs. Use of a non-borehole compensated sonic logging tool may lead to errors due to travel path distortion and cycle skipping. Uncertainties related to calibration and pen adjustments on parts of the resistivity logs also introduced errors. Nevertheless, patterns similar to those observed from deep well data can be discerned.

An important feature clearly evident on the graphs are offset groups of points. A separate scale function relating transit time and resistivity can be obtained from each group of points. The different groups are observed to correspond to differences in the chlorinity of the formation water. The groups are offset from one another because salinity, which is directly proportional to chlorinity, has a much greater influence on resistivity than on transit time. The results of this study indicate

that it is essential to consider the salinity of the formation water as well as electrical resistivity for purposes of calculating pseudosonic logs.

In the analysis of Rudman (1984) three constant coefficients must be determined experimentally to obtain an empirical scale function. Reasonable results were obtained because the measurements used in that effort were made in a zone where the salinity of the formation water was more or less constant. The present study suggest that it may be possible to replace these constants with chlorinity dependent coefficients. Seemingly consistent results were obtained using data from sections of carbonate rock. However, limited data from sections of clastic rock indicate that the scale function required to calculate pseudosonic logs for these sections is different from the scale function applicable in carbonate sections.

The pseudosonic logs obtained for the four wells used in this study display considerable variations in quality. In some sections detailed features of sonic logs were reproduced, while in other sections the pseudosonic log compared poorly with the sonic log. These results indicate that reasonably reliable pseudosonic logs can be obtained only by using high quality electrical resistivity logs from wells where information about the salinity of the formation water is also available.

To obtain pseudosonic logs with detail comparable to a conventional sonic log it appears to be necessary to use focused electrical logs. If unfocused logs must be used, the corresponding sonic and electrical logs used to determine the scale function should both be smoothed by some means such as a running average to attempt to minimize the distortion of resistivity measurements caused by thin beds.

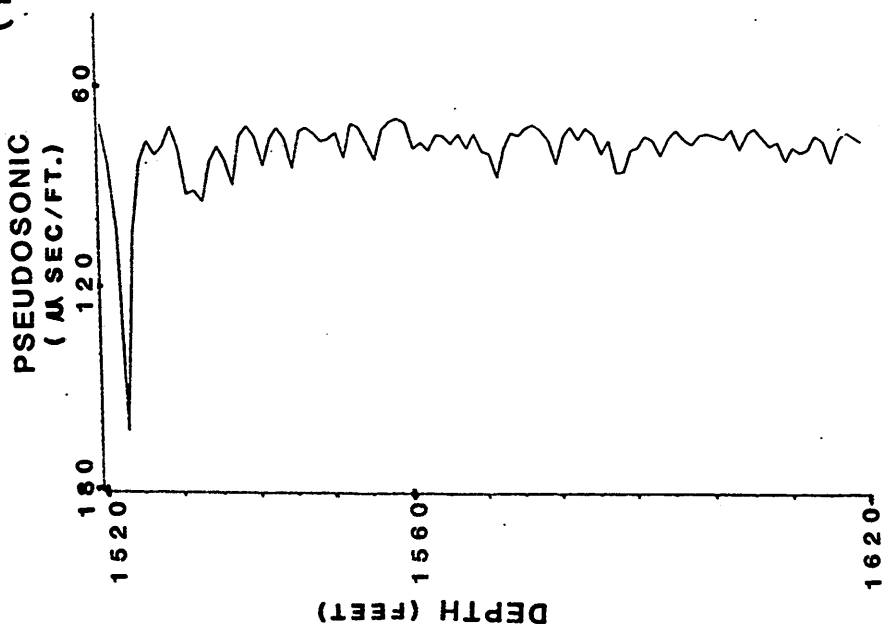
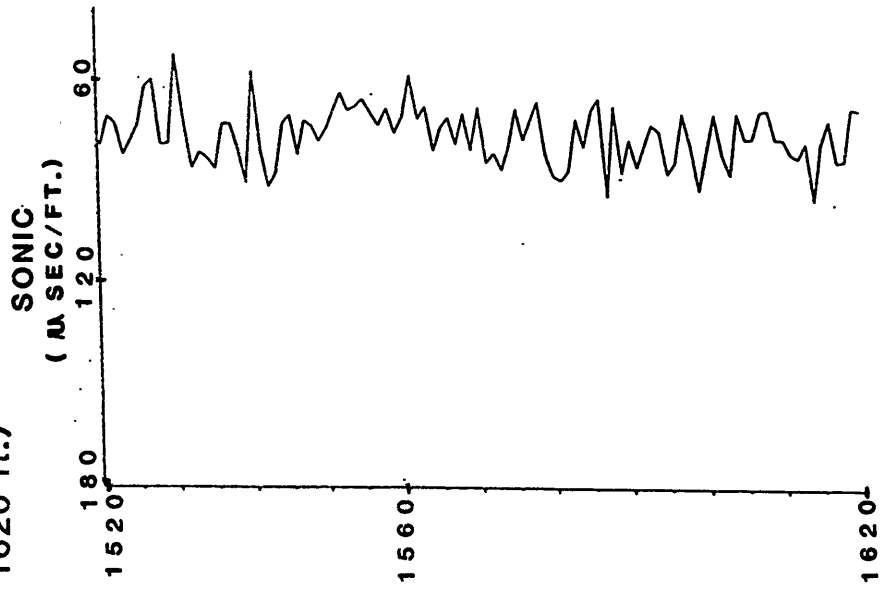
BIBLIOGRAPHY

- Archie, G. E., 1942, The electrical resistivity log as an aid in determining some reservoir characteristics: AIME Trans. - Petroleum Development and Technology, v. 146, p. 54-62.
- Asquith, G. B., and Gibson, C. R., 1982. Basic Well Log Analysis For Geologists: A.A.P.G., Oklahoma, 216 p.
- Bonner, B. P., and Schock, R. N., 1981, Seismic Wave Velocity: Handbook of physical properties of rocks and minerals, v. II-2, p. 221-256.
- Gill, H., and Mitchell, G., 1979, Investigations of Alternative Sources of Groundwater in the Coastal area of Georgia - Results of Colonels Island Deep Hydrologic Test Well, Appendix C: U.S. Geol. Survey Open-File Report 80-3, C1-C13.
- Gregg, D. O., and Zimmerman, E. A., 1974, Geologic and Hydrologic Control of Chloride Contamination in aquifers at Brunswick, Glynn County, Georgia: U.S. Geol. Water-Supply Paper 2029-D, p. D1-D44.
- Kim, D. Y., 1964, Synthetic velocity log: Paper presented at 33rd Annual Intern. SEG Meeting, New Orleans.
- Knauss, J. A., 1968. Introduction to Physical Oceanography: Prentice-Hall, Inc., 338 p.
- Krauss, R. E., Matthews, S. E., and Gill, H. E., 1984, Evaluation of the ground-water resources of Coastal Georgia - Preliminary report on the data available as of July 1983: Georgia Geologic Survey Information Circular 62, 55 p.
- Lynch, E.J., 1962. Formation Evaluation: Harper & Row, Publishers, 422 p.
- Olhoeft, G. R., 1981, Electrical properties of rocks: Handbook of physical properties of rocks and minerals, v. II-2, p. 257-329.
- Press, F., 1966, Seismic velocities, in Handbook of Physical Constants, Ed. S. P. Clark, GSA Mem. 97, p.195-218.

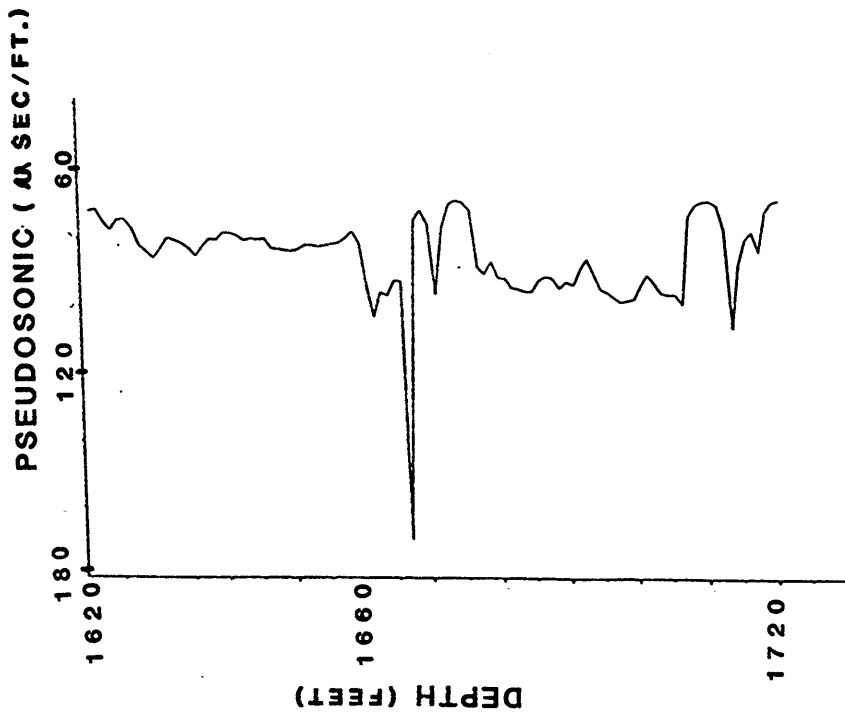
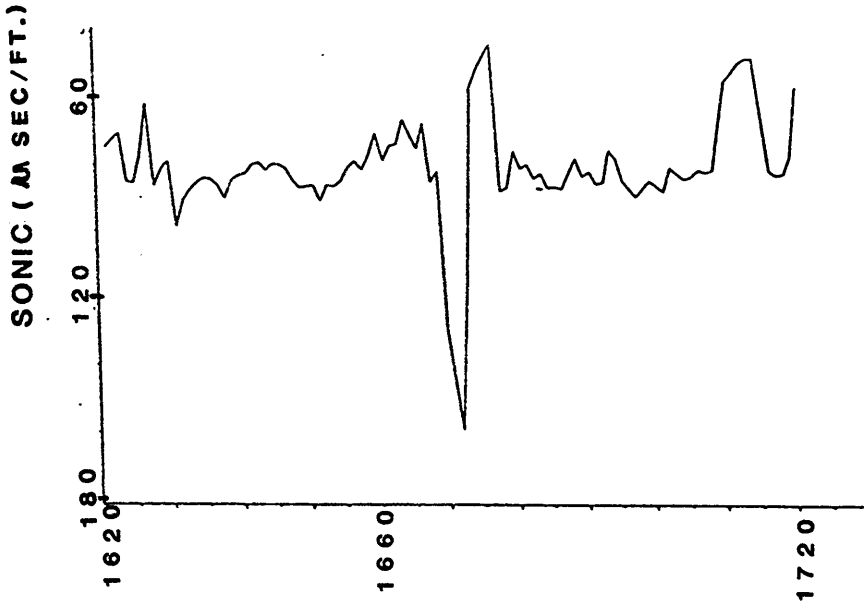
- Press, W. H., Flannery, B. P., Teukolsky, S. A., and Vetterling, W. T., 1988 ed., Numerical Recipes: The Art of Scientific Computing: Cambridge University Press, pp. 484 - 486.
- Rudman, A. J., Whaley, J. F., Blakely, R. F., and Biggs, M. E., 1975, Transformation of resistivity to pseudovelocity logs, AAPG Bull., 59, p. 1151-65.
- Rudman, A. J., 1984, Interrelationship of resistivity and velocity logs: Developments in Geophysical Exploration Methods - 3, v. 3, p. 33-59.
- Schlumberger Limited, 1972 ed., Log Interpretation: Volume I - Principles, 113 p.
- Serra, O., 1984, Fundamentals of well-log interpretation: 1.the acquisition of logging data: Elsevier Publishers, 423 p.
- Stiles, H.R., and Matthews, S.E., 1983, Ground-Water data for Georgia, 1982: U.S. Geol. Survey Open-File Report 83-678, 147 p.
- Telford, W. M., Geldart, L. P., Sheriff, R. E., and Keys, D. A., 1976. Applied Geophysics: Cambridge University Press, 860 p.
- Wait, R. L., and Gregg, D. O., 1973, Hydrology and Chloride Contamination of the Principal Artesian aquifer in Glynn County, Georgia: U.S. Geological Survey Hydrologic Report 1, p. 1-90.
- Wylie, M. R. J., Gregory, H. R., and Gardner, L. W., 1956, Elastic waves in heterogeneous and porous media, Geophysics, v. 21, p. 41-70.

**Appendix A. PSEUDOSONIC AND SONIC
LOGS FOR ALL FOUR TEST WELLS IN
BRUNSWICK, GEORGIA.**

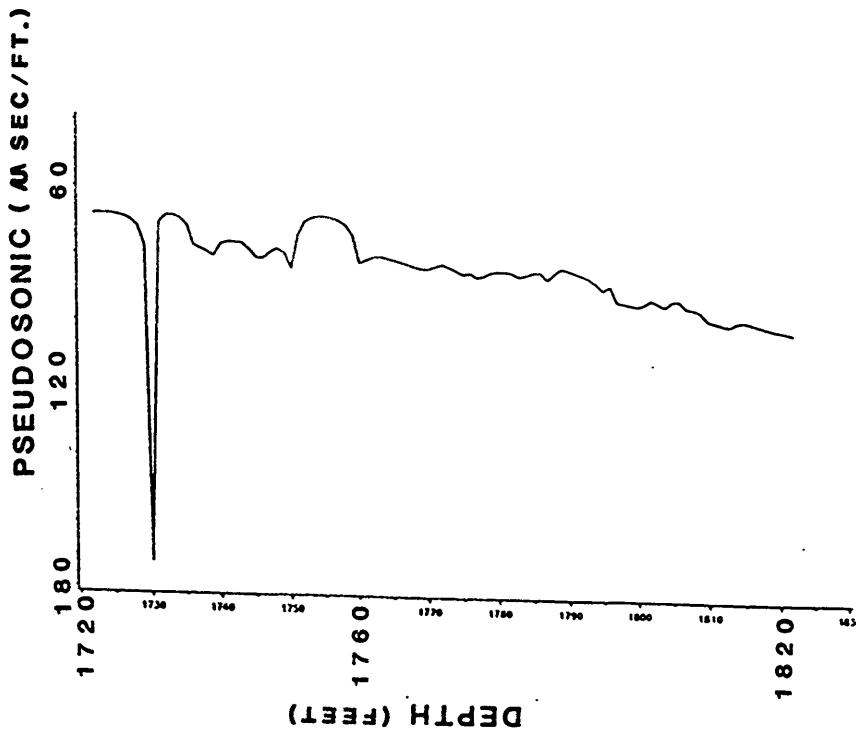
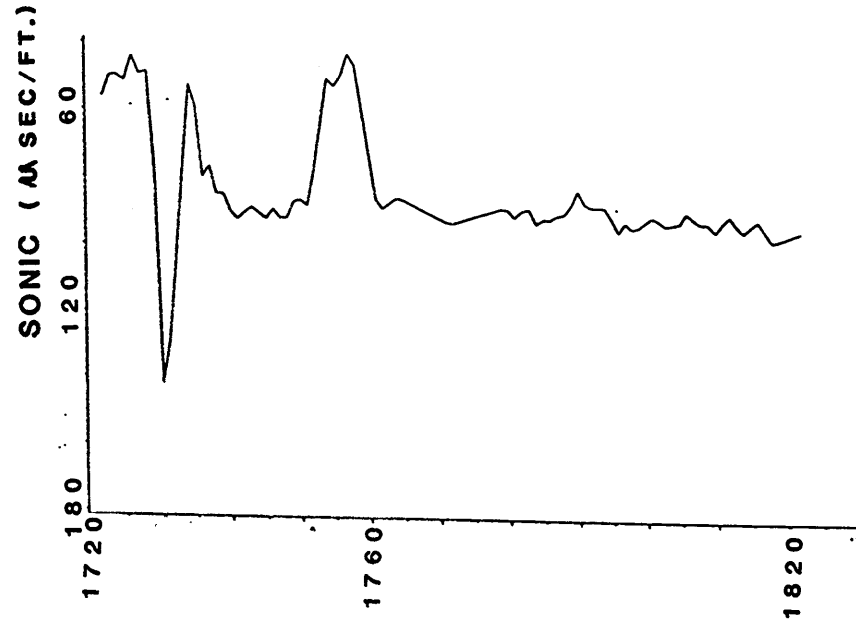
TW26
(1520 - 1620 ft.)



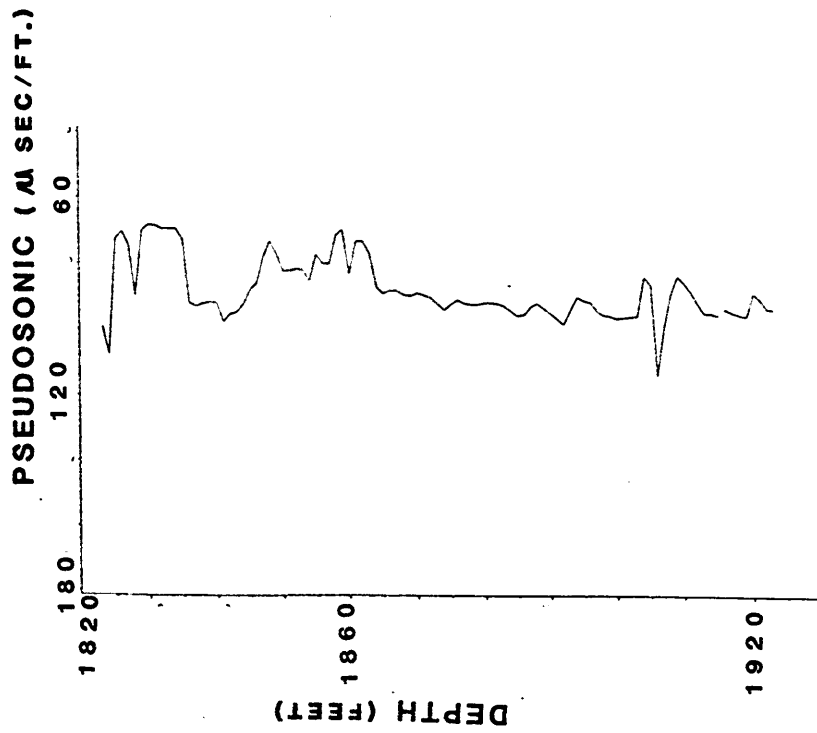
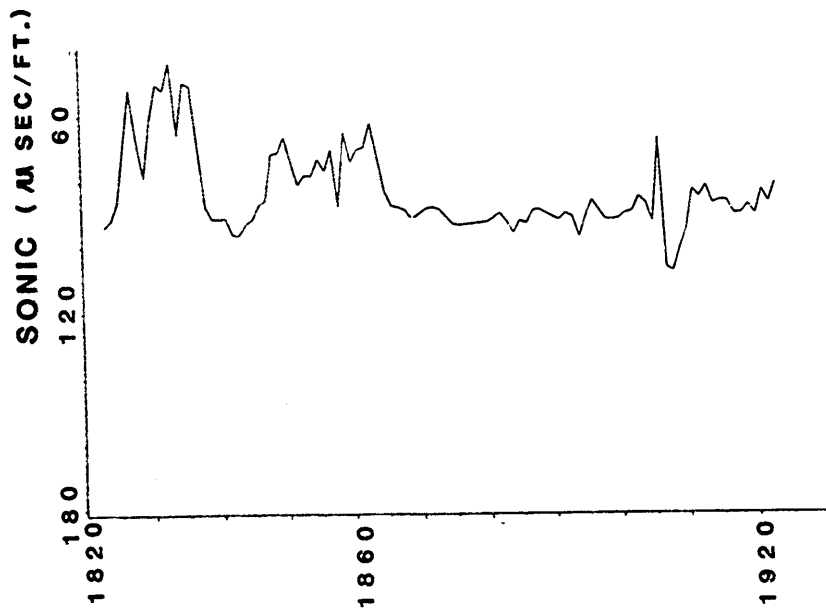
TW26
(1620 - 1720 ft.)



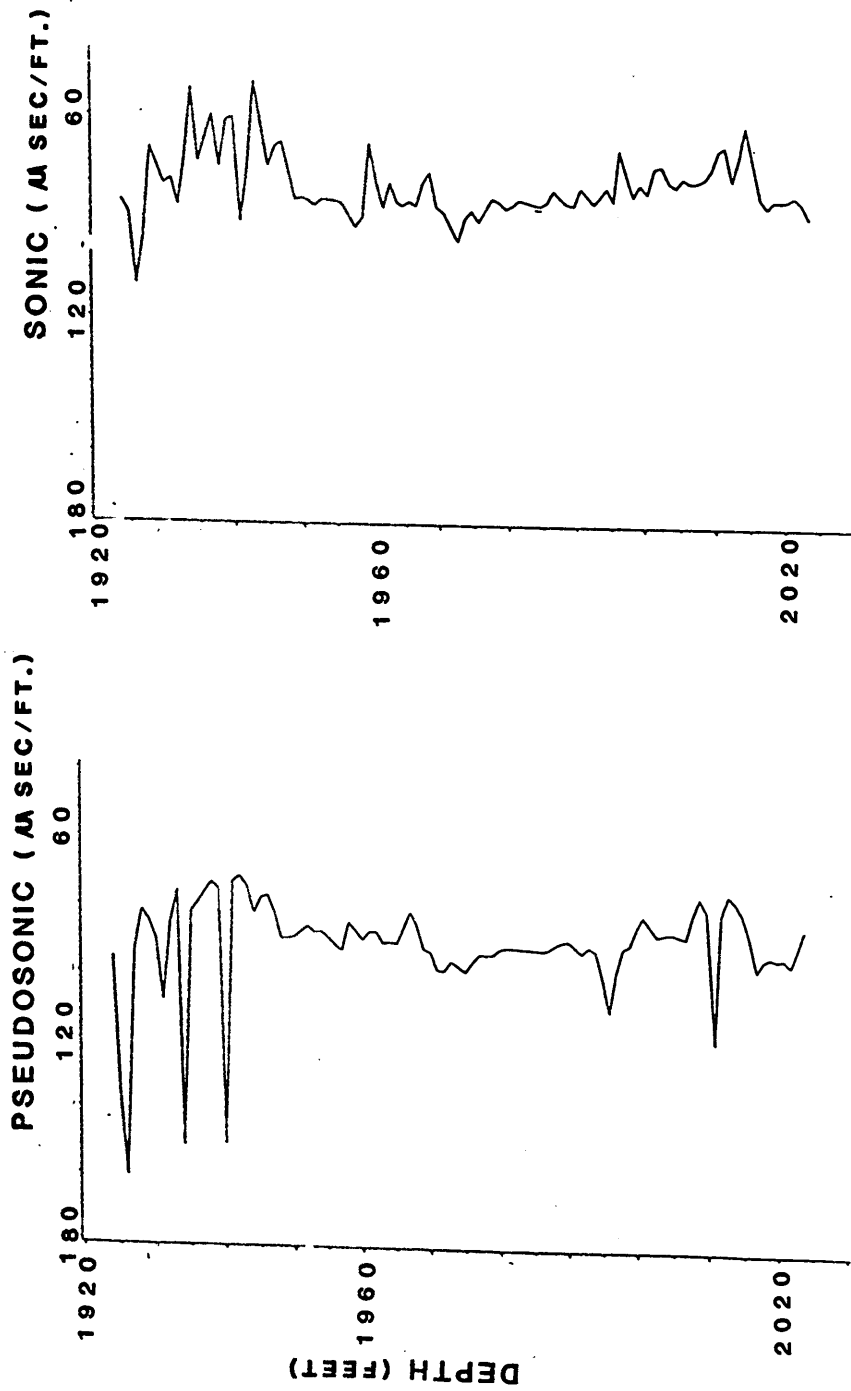
TW26
(1720 - 1820 ft.)



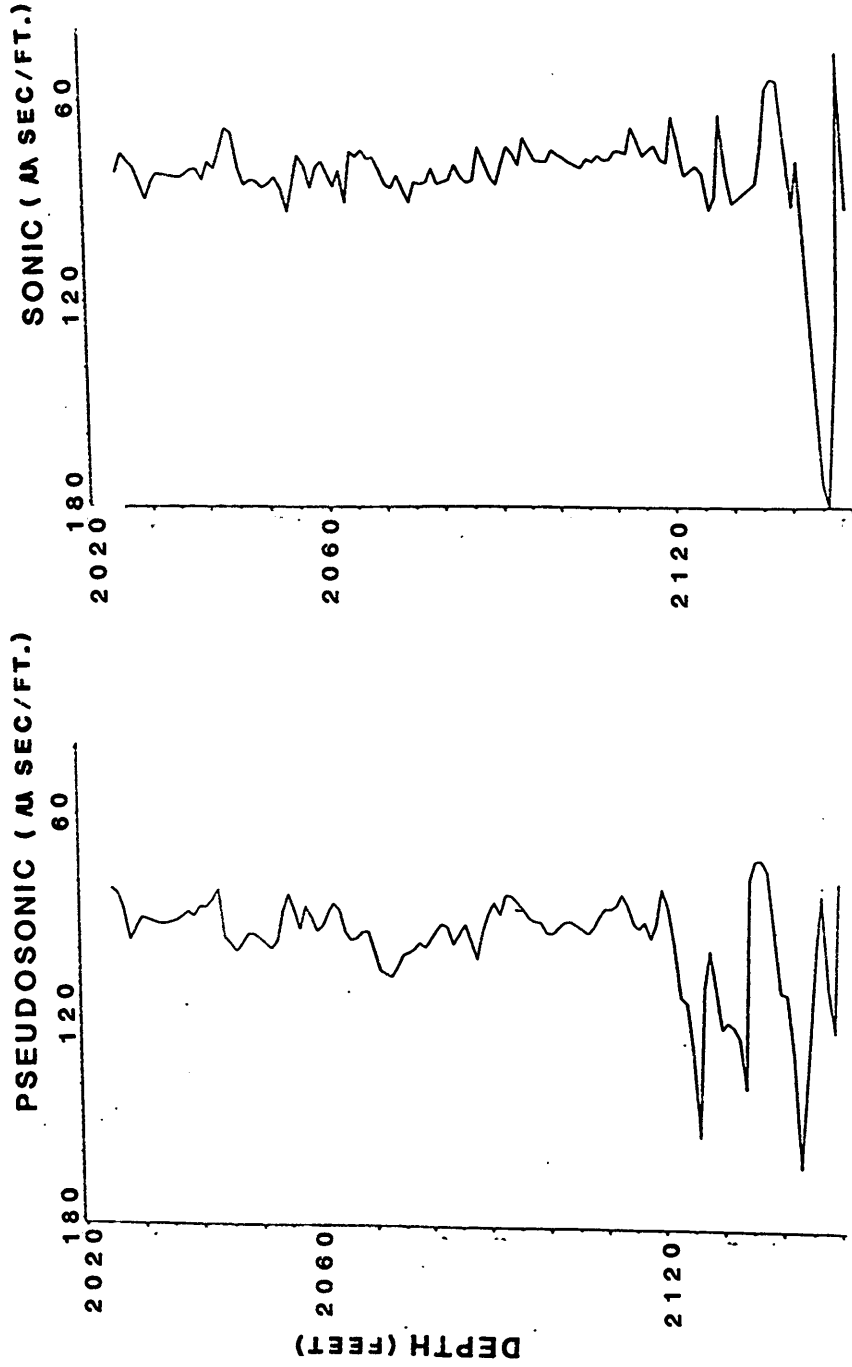
TW26
(1820 - 1920 ft.)



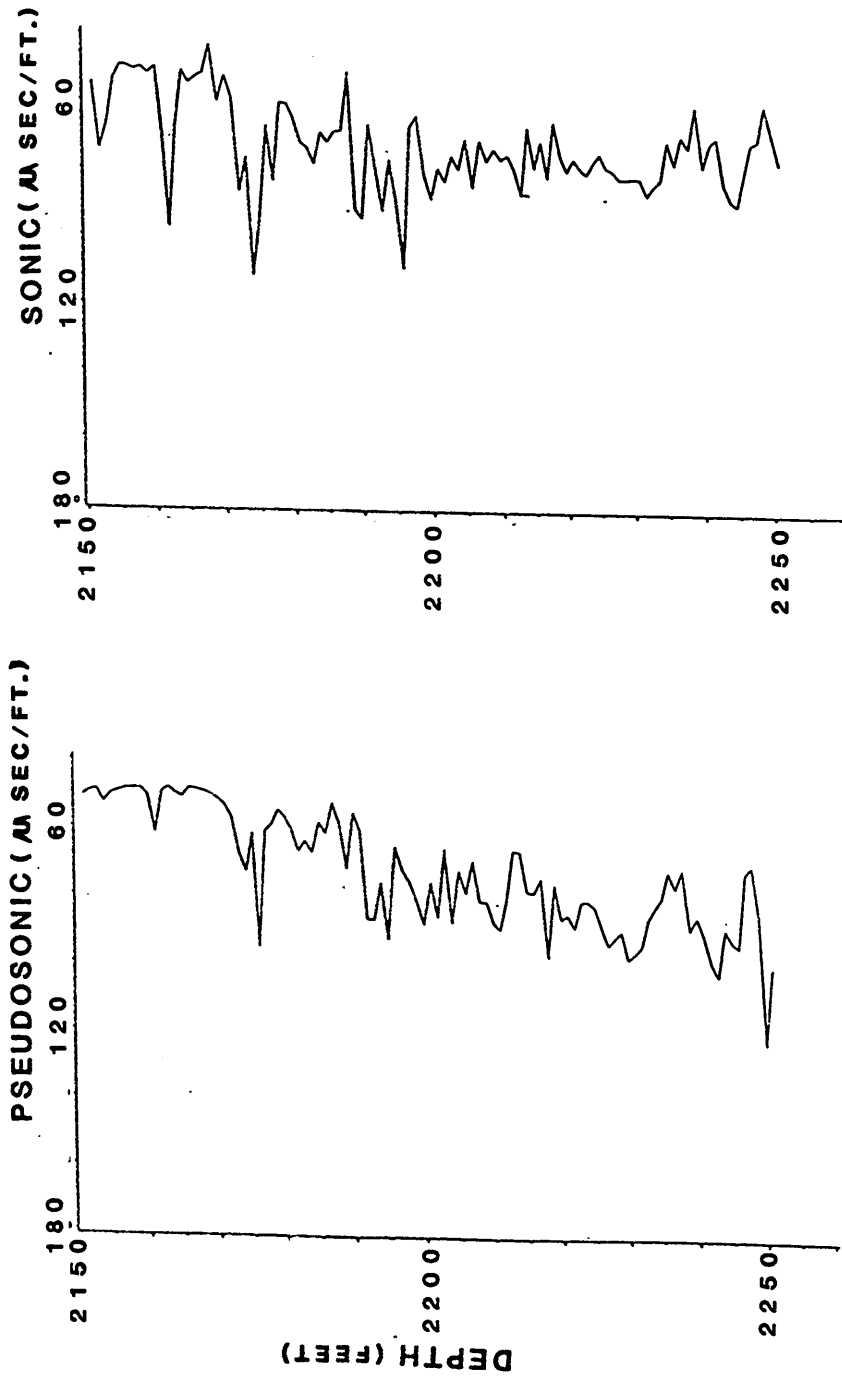
TW26
(1920 - 2020 ft.)



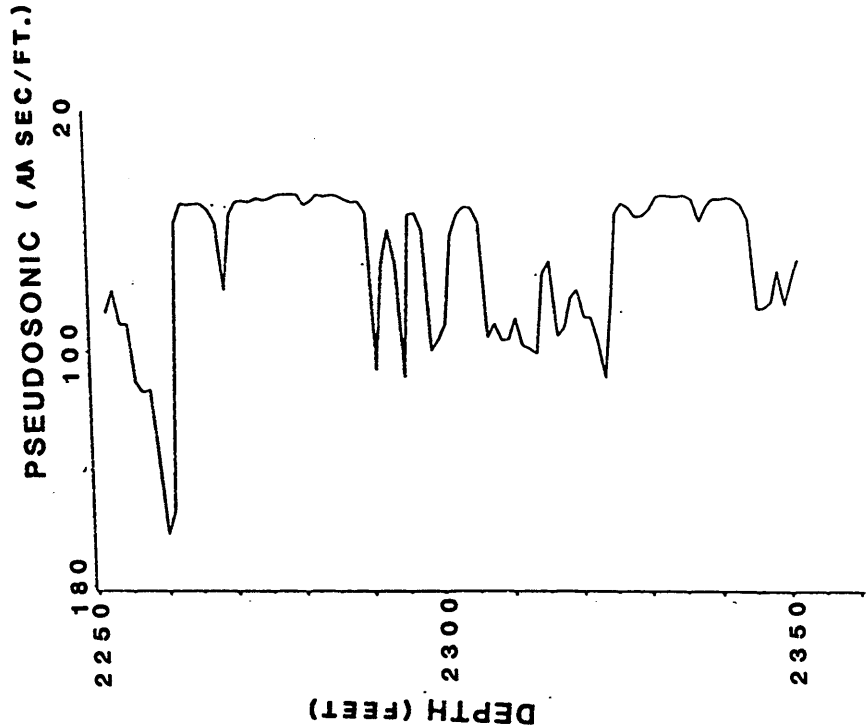
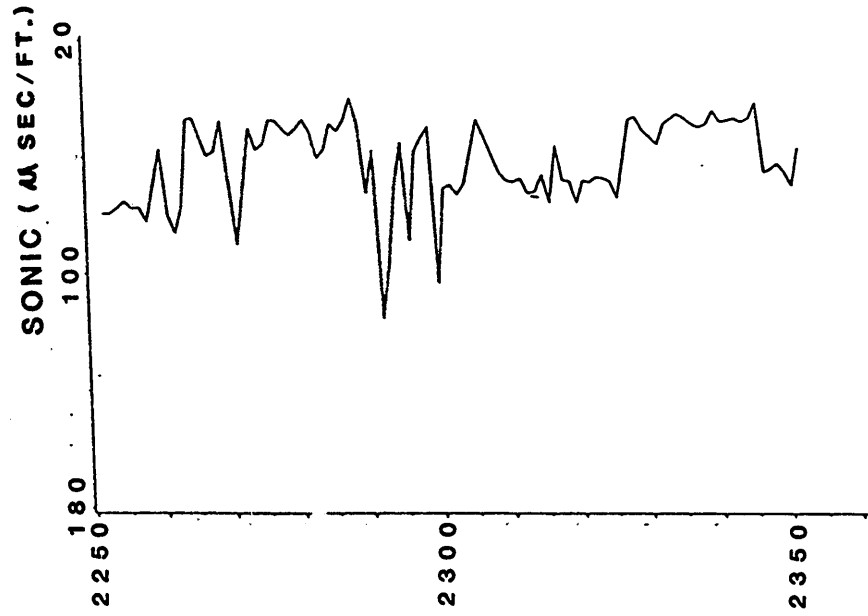
TW26
(2020 - 2150 ft.)



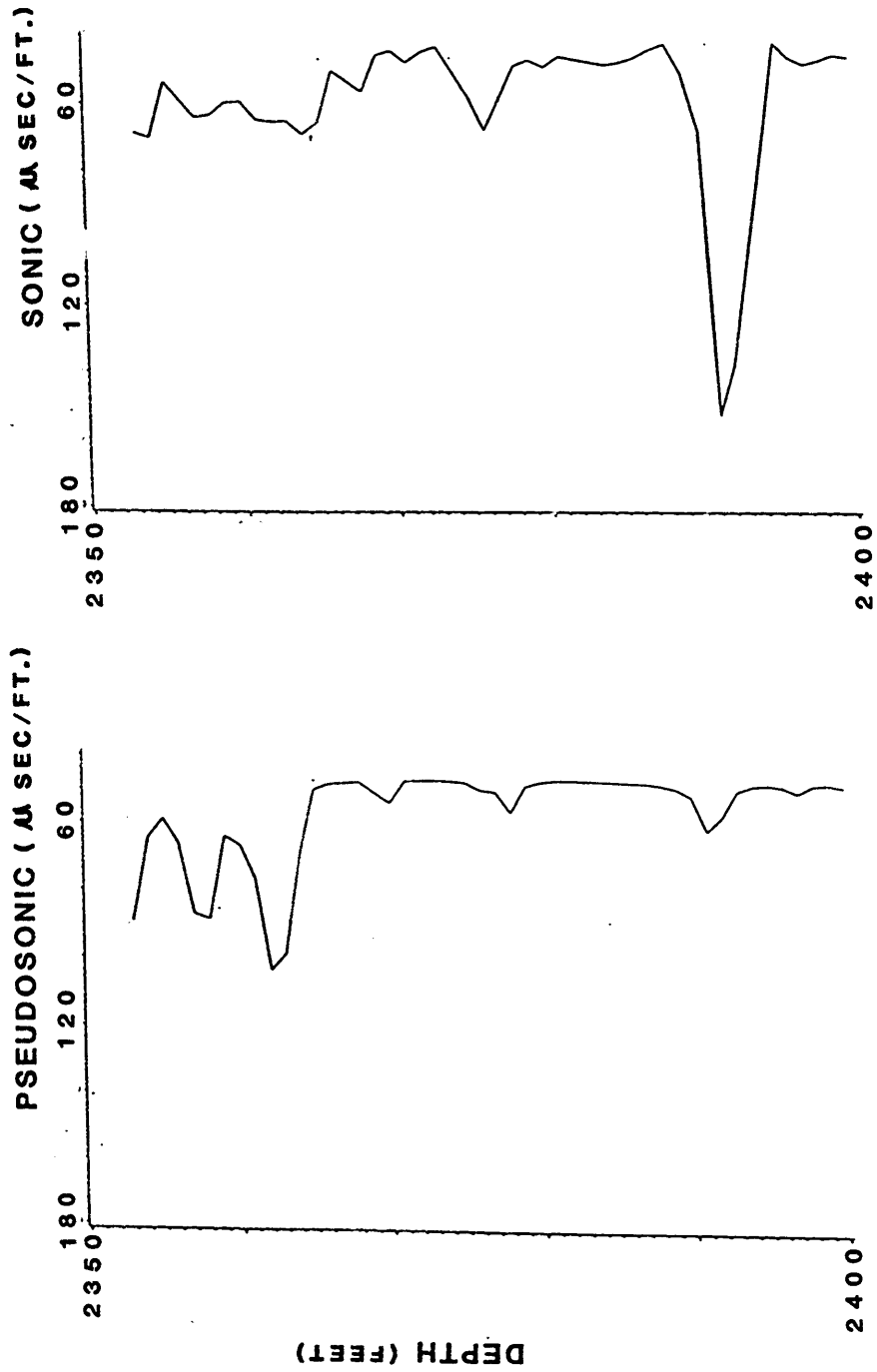
TW26
(2150 - 2250 ft.)



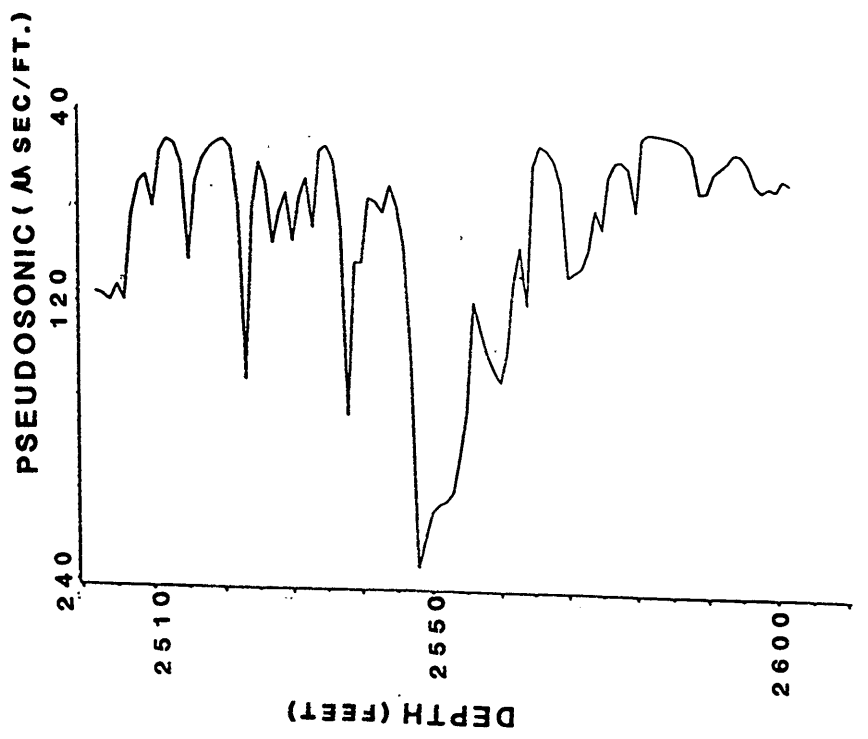
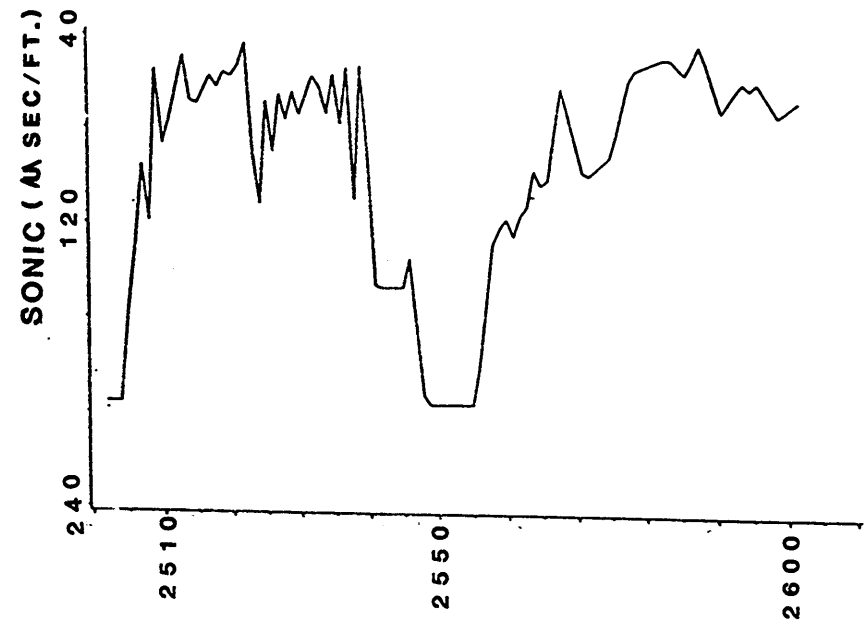
TW26
(2250 - 2350 ft.)



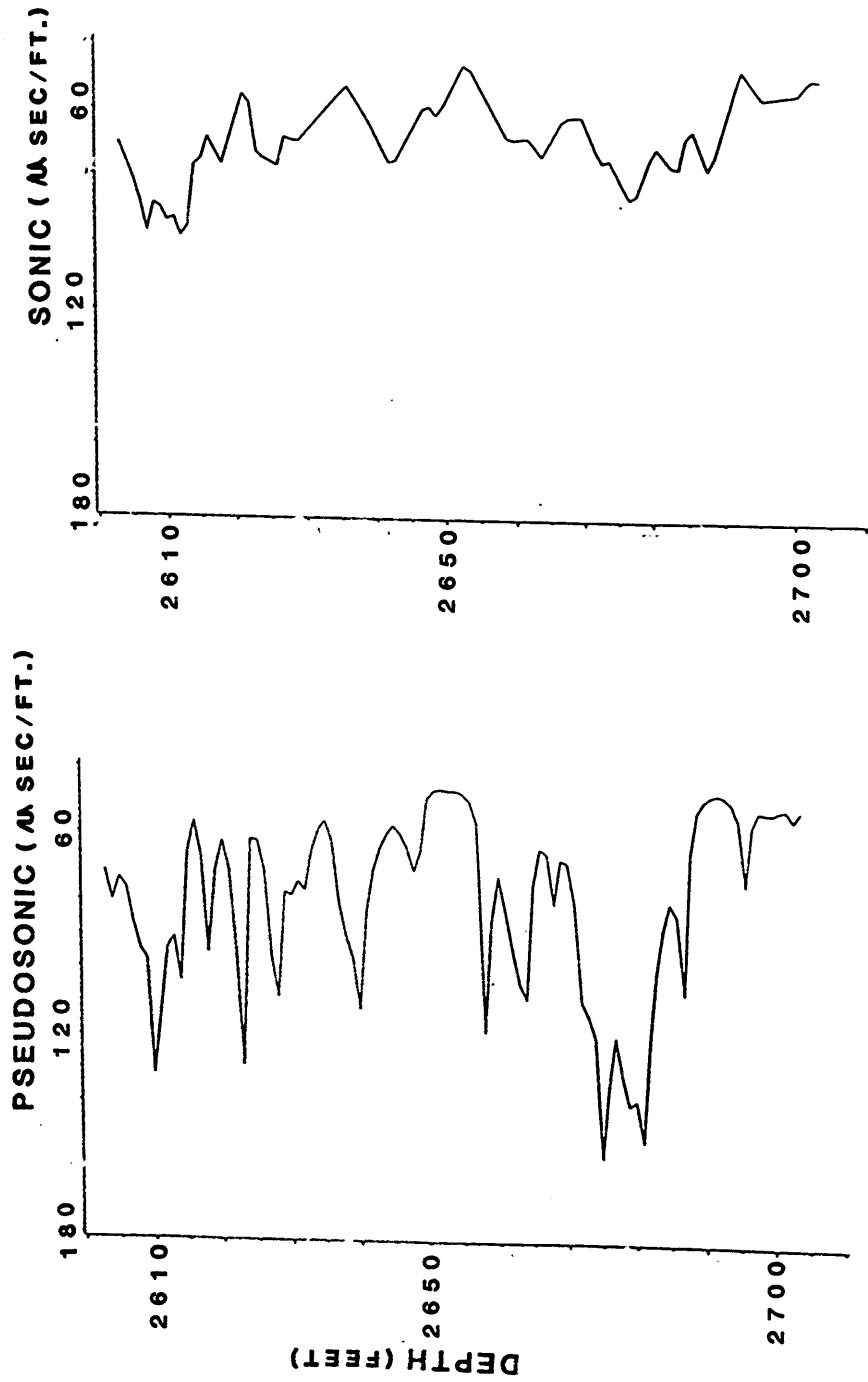
TW26
(2350 - 2400 ft.)



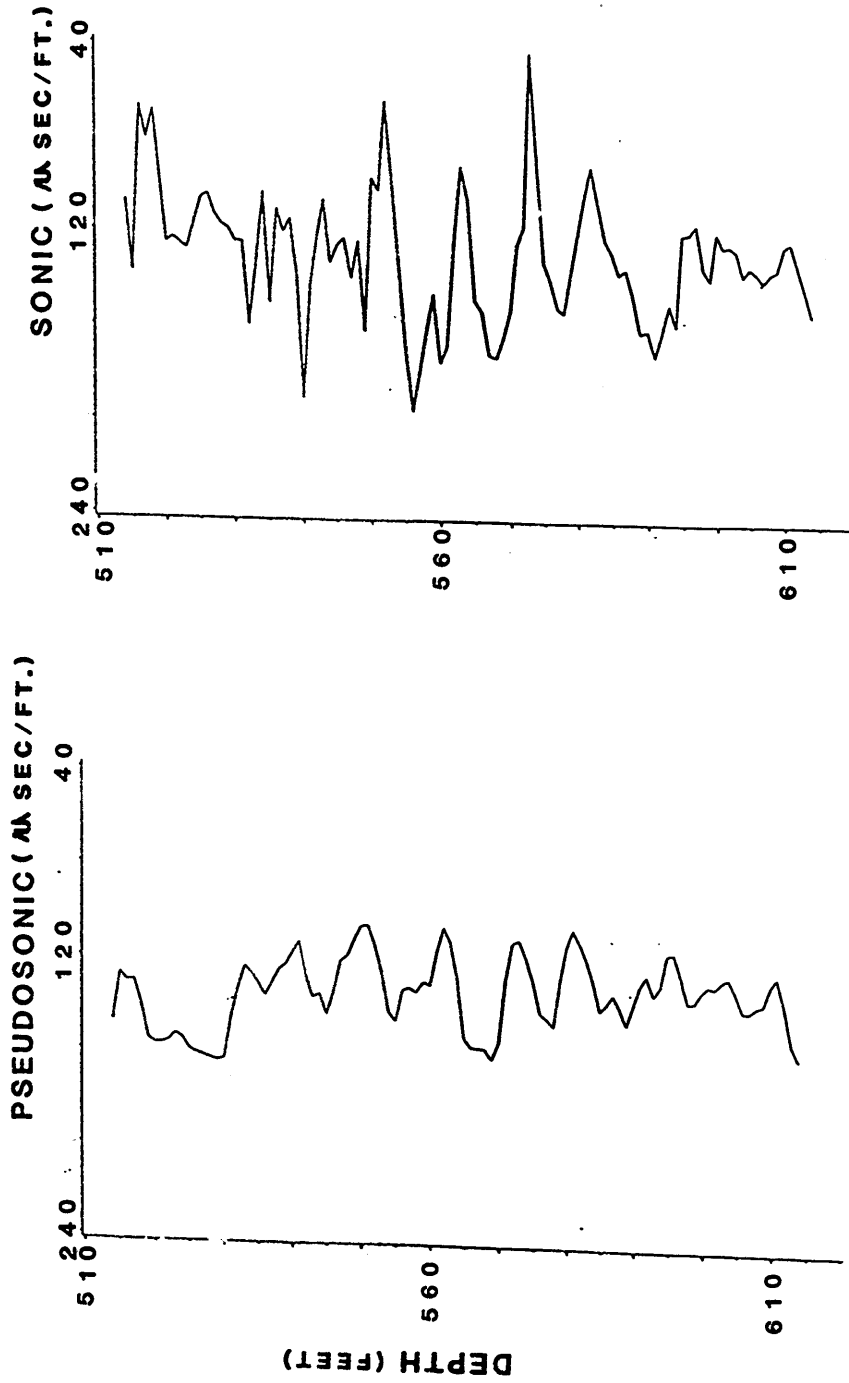
TW26
(2510 - 2610 ft.)



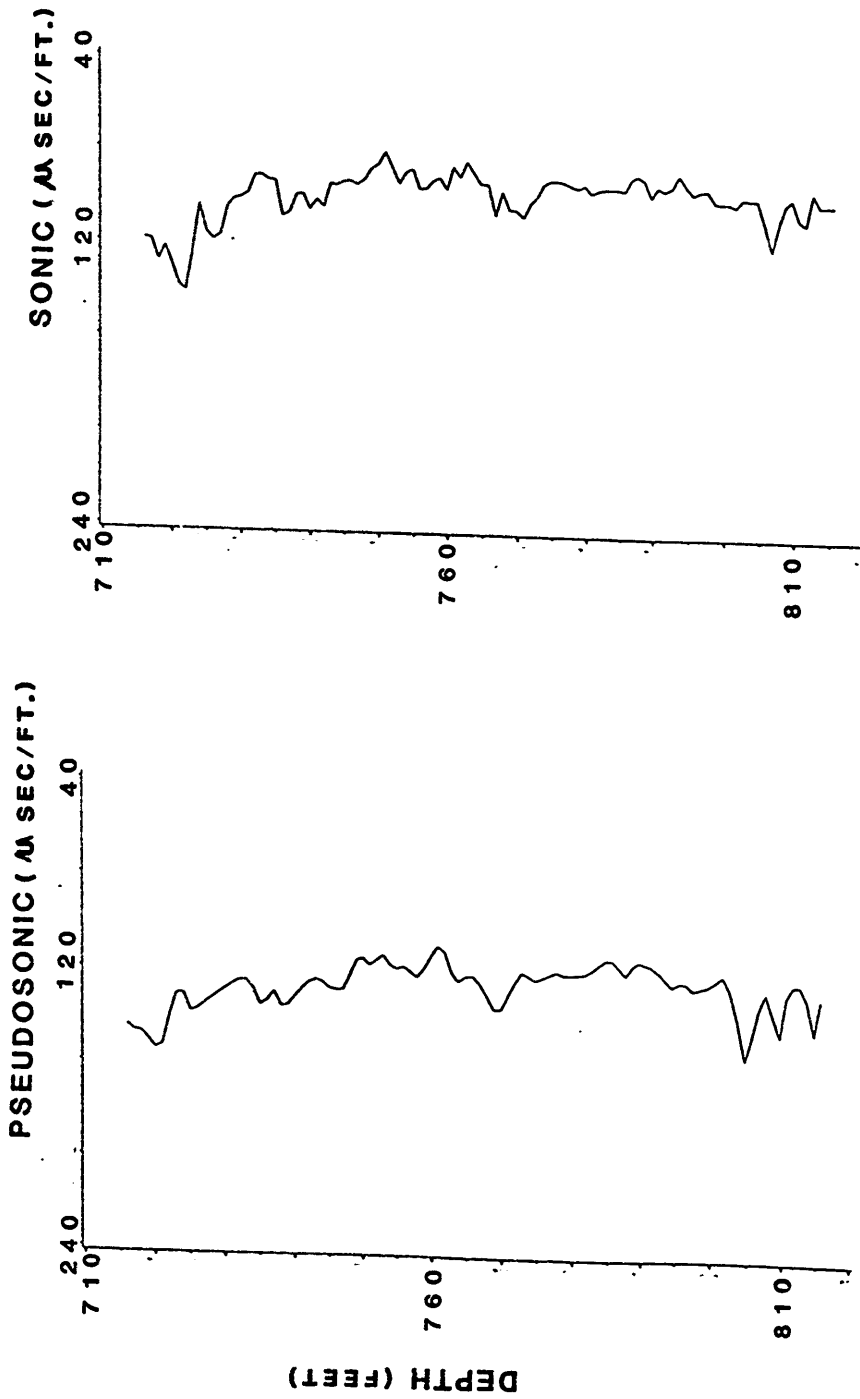
TW26
(2610 - 2710 ft.)



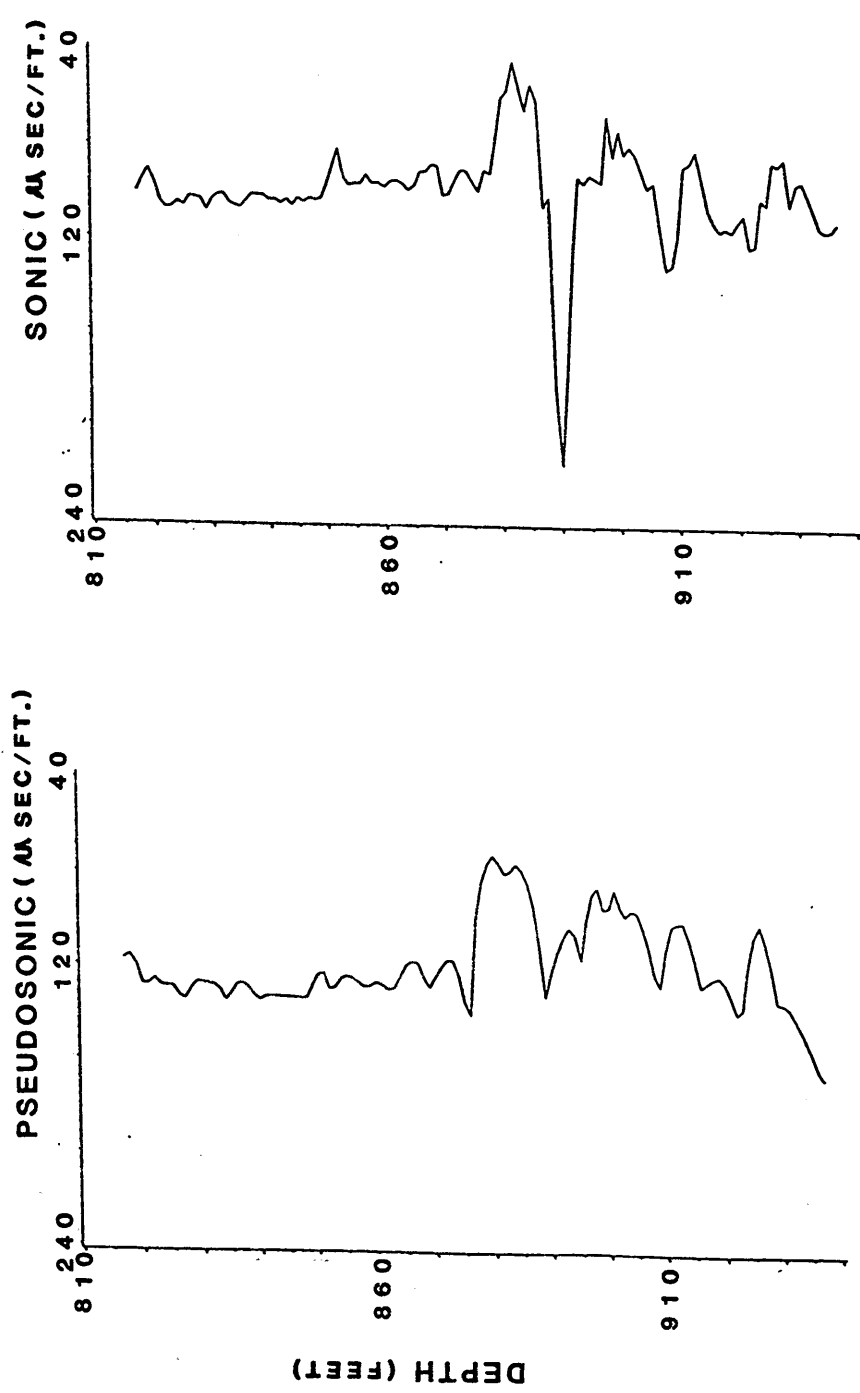
GRANT ST.
(510 - 610 ft.)



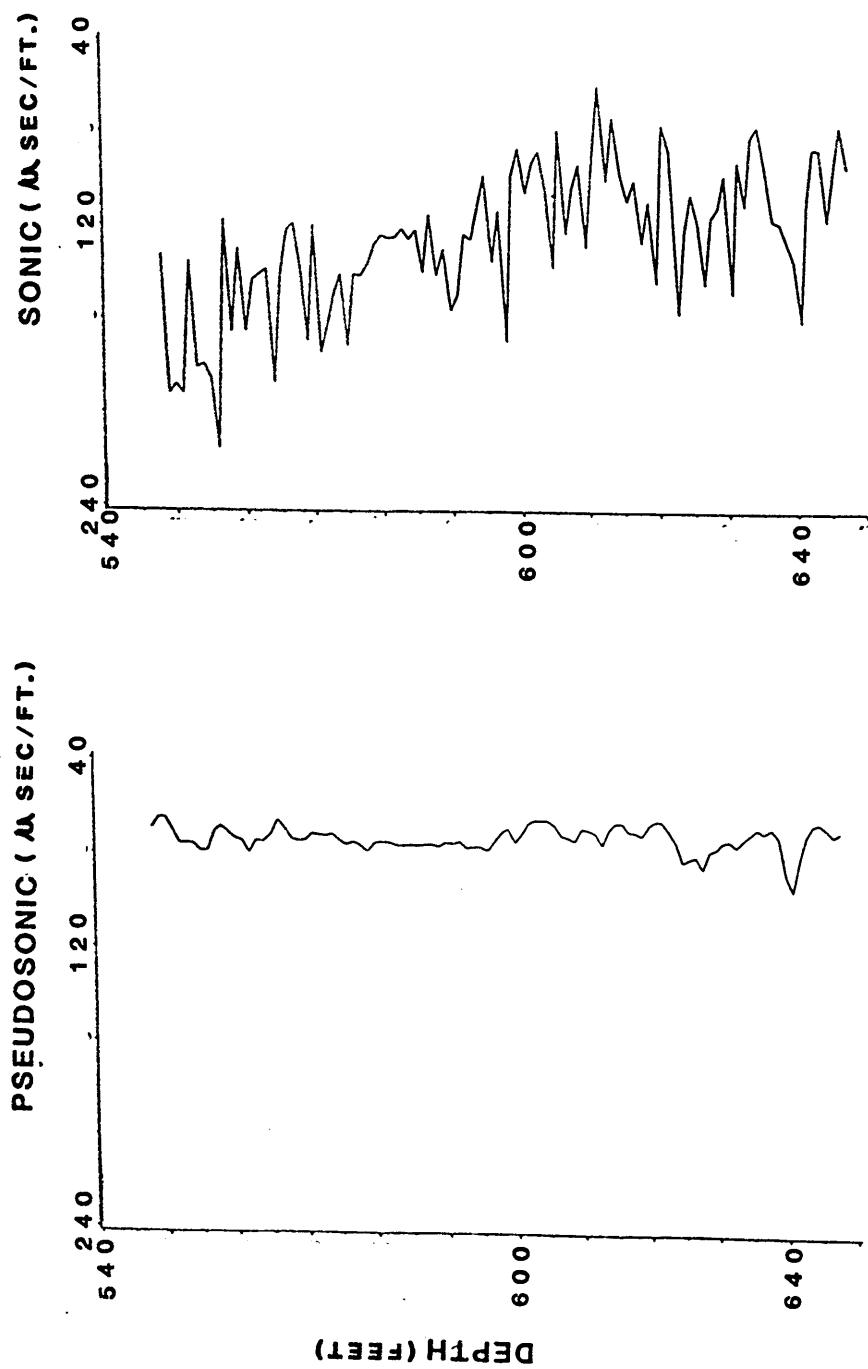
GRANT ST.
(710 - 810 ft.)



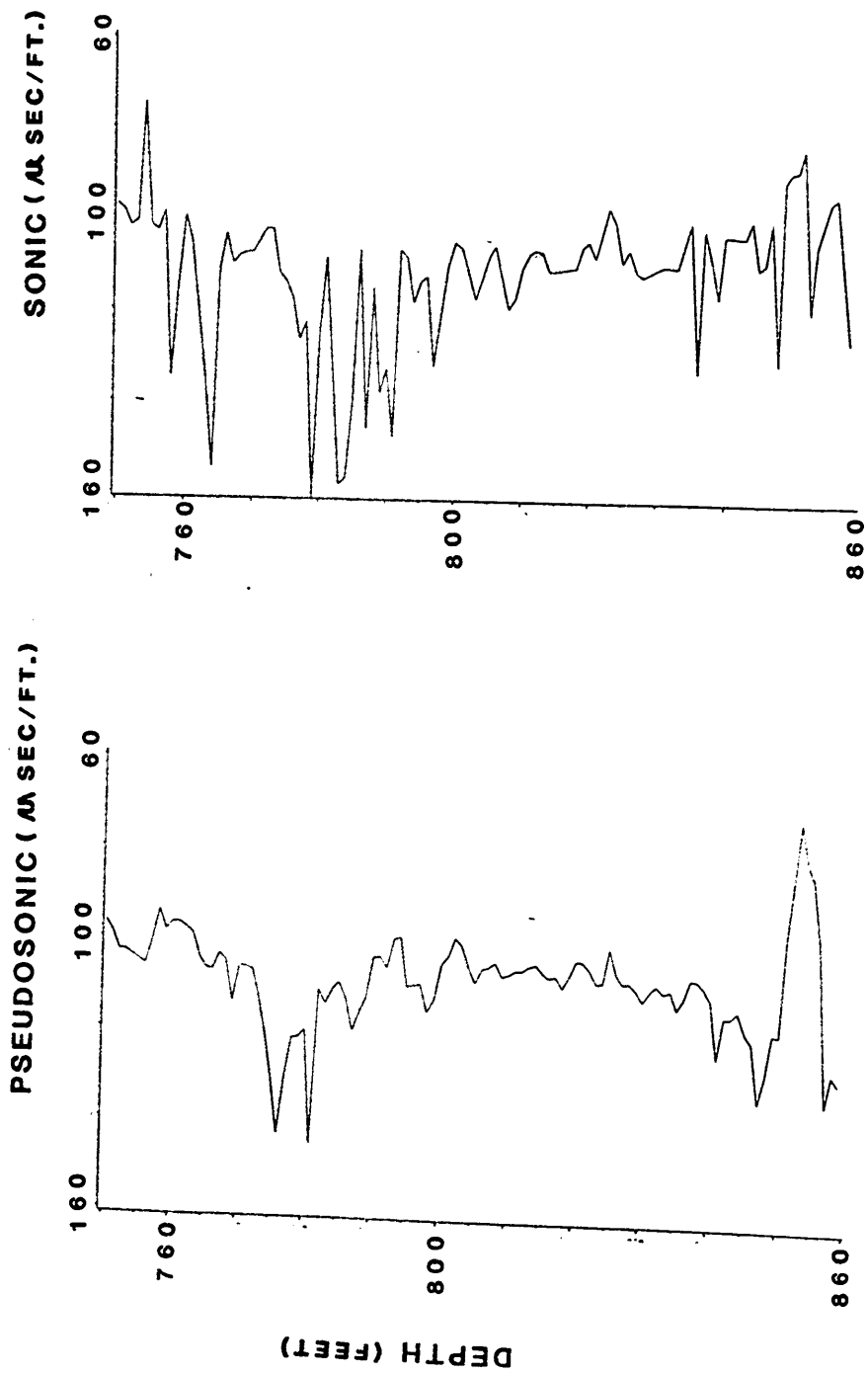
GRANT ST.
(810 - 940 ft.)



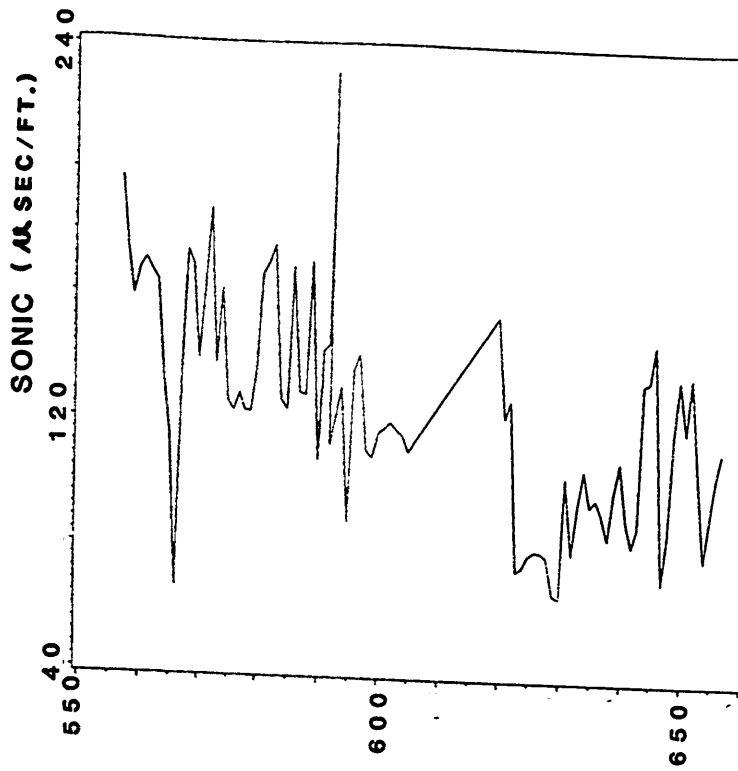
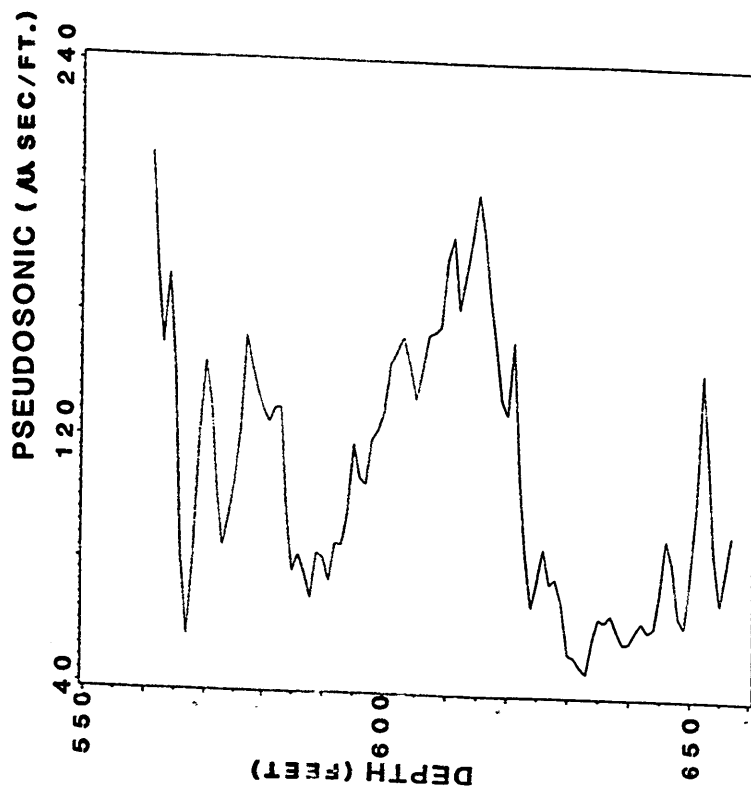
HERCULES 'O'
(540 - 640 ft.)



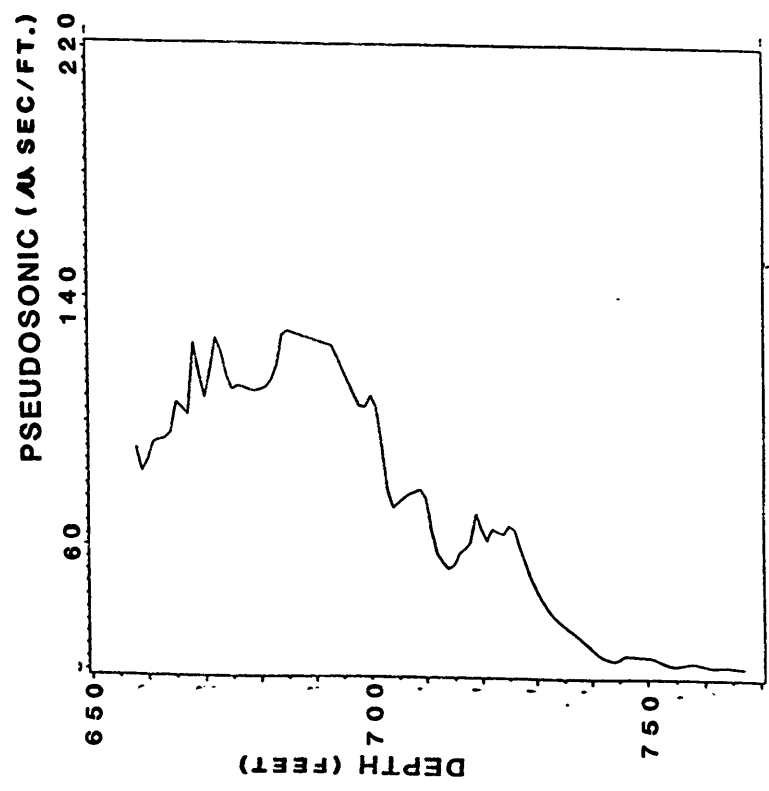
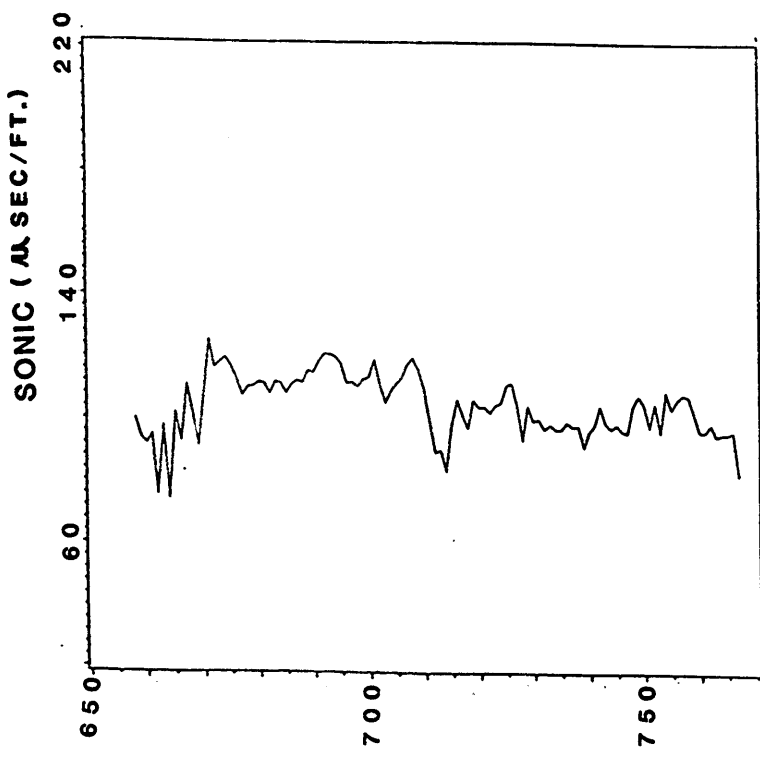
HERCULES 'O'
(740 - 860 ft.)



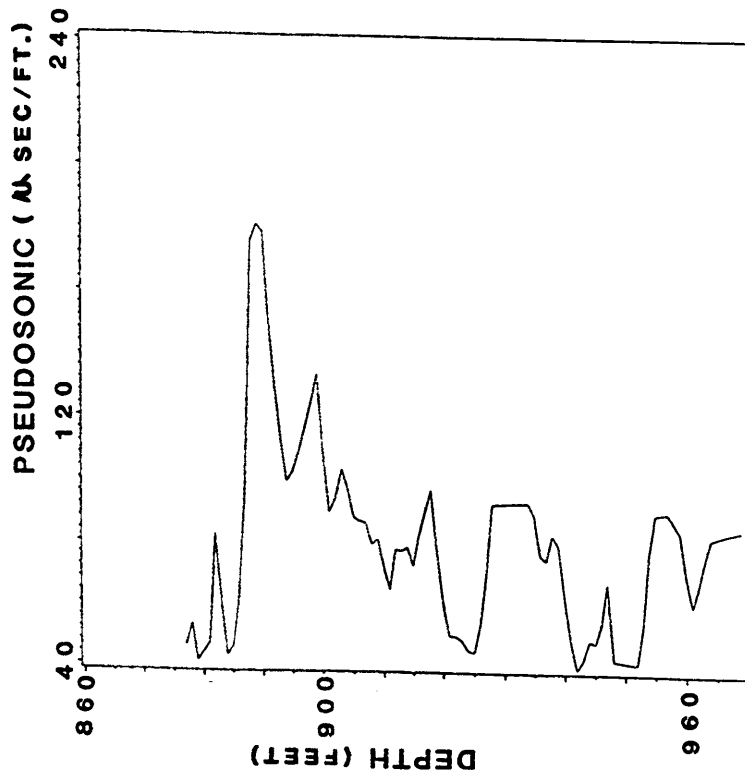
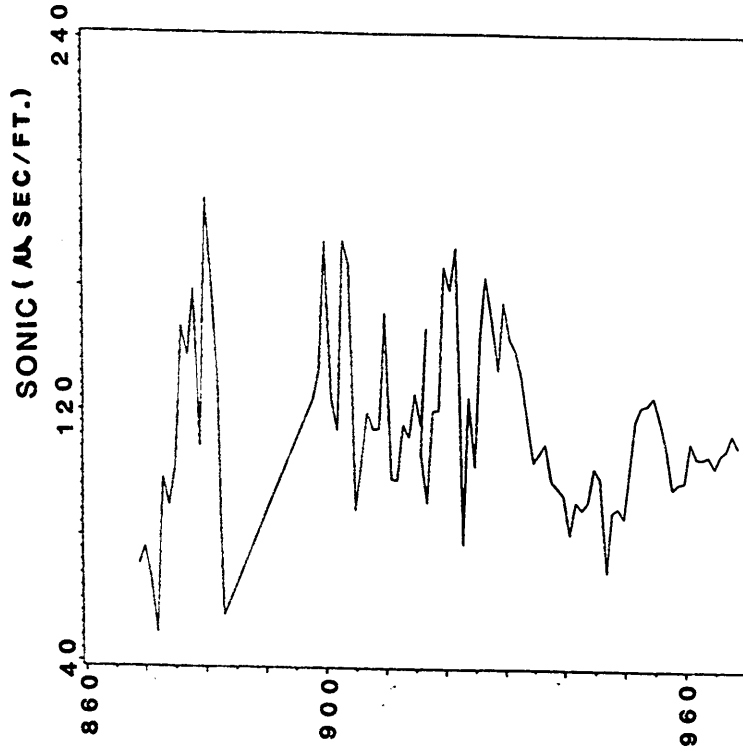
BP&P NO. 10
(550 - 660 ft.)



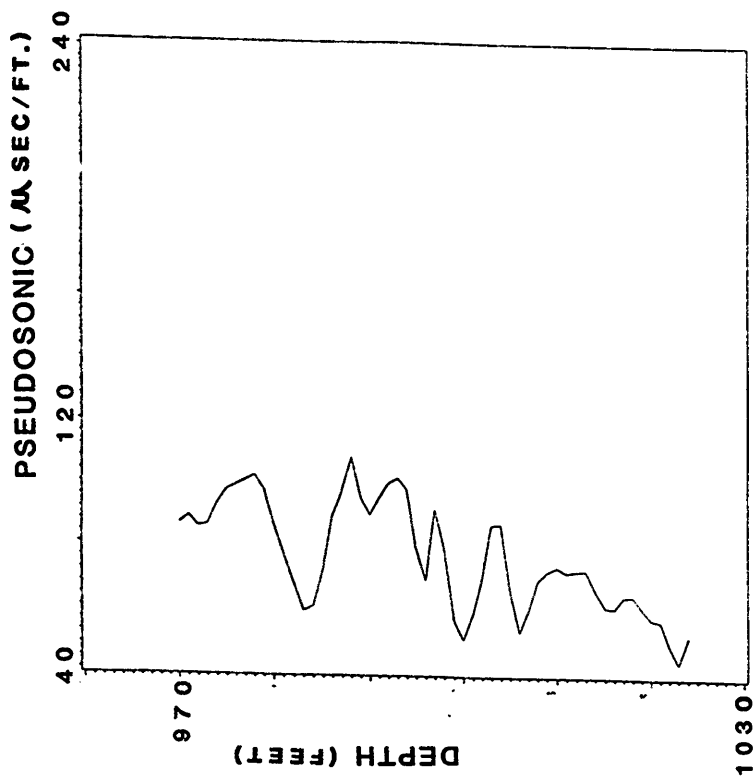
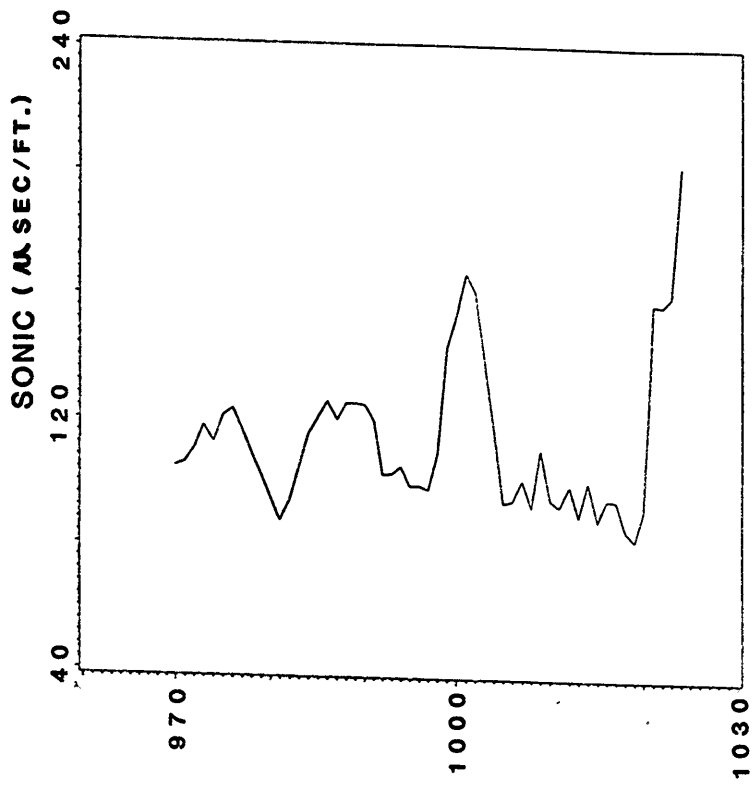
BP&P NO. 10
(650 - 770 ft.)



BP&P NO. 10
(860 - 970 ft.)



BP&P NO. 10
(970 - 1030 ft.)



**The vita has been removed from
the scanned document**